

# Research status of supercritical aviation kerosene and a convection heat transfer considering thermal pyrolysis

Supercritical  
aviation  
kerosene

3039

Yong Li and Yingchun Zhang

*School of Mechanical Engineering, Northwestern Polytechnical University, Xi'an, China; School of Marine Science and Technology, Northwestern Polytechnical University, Xi'an, China and Department of Energy Sciences, Lund University, Lund, Sweden*

Gongnan Xie

*School of Marine Science and Technology, Northwestern Polytechnical University, Xi'an, China and Research and Development Institute of Northwestern Polytechnic, University of Shenzhen, Shenzhen, China, and*

Bengt Ake Sunden

*Department of Energy Sciences, Lund University, Lund, Sweden*

Received 23 August 2021  
Revised 5 December 2021  
Accepted 15 December 2021

## Abstract

**Purpose** – This paper aims to comprehensively clarify the research status of thermal transport of supercritical aviation kerosene, with particular interests in the effect of cracking on heat transfer.

**Design/methodology/approach** – A brief review of current research on supercritical aviation kerosene is presented in views of the surrogate model of hydrocarbon fuels, chemical cracking mechanism of hydrocarbon fuels, thermo-physical properties of hydrocarbon fuels, turbulence models, flow characteristics and thermal performances, which indicates that more efforts need to be directed into these topics. Therefore, supercritical thermal transport of n-decane is then computationally investigated in the condition of thermal pyrolysis, while the ASPEN HYSYS gives the properties of n-decane and pyrolysis products. In addition, the one-step chemical cracking mechanism and SST  $k-\omega$  turbulence model are applied with relatively high precision.

© Yong Li, Yingchun Zhang, Gongnan Xie and Bengt Ake Sunden. Published by Emerald Publishing Limited. This article is published under the Creative Commons Attribution (CC BY 4.0) licence. Anyone may reproduce, distribute, translate and create derivative works of this article (for both commercial and non-commercial purposes), subject to full attribution to the original publication and authors. The full terms of this licence may be seen at <http://creativecommons.org/licences/by/4.0/legalcode>

This work was sponsored by the National Natural Science Foundation of China (51676163), the National 111 Project under Grant No. B18041, the Fundamental Research Funds of Shenzhen City (JCYJ20170306155153048) and the Innovation Foundation for Doctor Dissertation of Northwestern Polytechnical University under Grant No. CX202029. This research work was also financially supported by the China Scholarship Council (CSC) giving Mr Yong Li the opportunity to perform part of his PhD studies at Lund University. The computations were performed on resources provided by the Swedish National Infrastructure for Computing (SNIC) at LUNARC and partially funded by the Swedish Research Council.



**Findings** – The existing surrogate models of aviation kerosene are limited to a specific scope of application and their thermo-physical properties deviate from the experimental data. The turbulence models used to implement numerical simulation should be studied to further improve the prediction accuracy. The thermal-induced acceleration is driven by the drastic density change, which is caused by the production of small molecules. The wall temperature of the combustion chamber can be effectively reduced by this behavior, i.e. the phenomenon of heat transfer deterioration can be attenuated or suppressed by thermal pyrolysis.

**Originality/value** – The issues in numerical studies of supercritical aviation kerosene are clearly revealed, and the conjugation mechanism between thermal pyrolysis and convective heat transfer is initially presented.

**Keywords** Heat transfer deterioration, Supercritical aviation kerosene, Thermal pyrolysis, Thermal-induced acceleration

**Paper type** Research paper

### Nomenclature

- $a$  = the size of a rectangular channel, mm;  
 $A$  = the area of the cross-section of the channel,  $m^2$ ;  
 $Bo^*$  = buoyancy factor;  
 $c_p$  = specific heat of the fluid, J/kg-K;  
 $c_s$  = volume concentration of component s,  $kmol/m^3$ ;  
 $C_R$  = reactant concentration,  $kmol/m^3$ ;  
 $d$  = hydraulic diameter of the circular pipe, m;  
 $D_s$  = the diffusion coefficient of the component s,  $m^2/s$ ;  
 $D_\omega$  = orthogonal divergence term;  
 $E_a$  = activation energy and its value is 263.7 kJ/mol;  
 $g$  = gravity acceleration,  $m/s^2$ ;  
 $g_i$  = gravitational volume force along the  $i$  direction,  $m/s^2$ ;  
 $G_k$  = term representing turbulent kinetic energy generated by laminar velocity gradient,  $m^2/s^2$ ;  
 $G_\omega$  = term representing turbulent kinetic energy generated by  $\omega$  equation,  $m^2/s^2$ ;  
 $Gr$  = Grashof number based on a temperature difference;  
 $k$  = turbulent kinetic energy,  $m^2/s^2$ ;  
 $k_0$  = pre-exponential factor and its value is  $1.6 \times 10^{15}$  1/s;  
 $K$  = reaction rate constant, 1/s;  
 $Kv$ : = acceleration parameter;  
 $L$  = length of the horizontal rectangular channel, mm;  
 $\bar{p}$  = operating pressure, Pa;  
 $\bar{p}$  = average pressure, Pa;  
 $Pr_t$  = turbulent Prandtl number;  
 $q_w$  = heat flux,  $kW/m^2$ ;  
 $q_m$  = mass flow rate, kg/s;  
 $R$  = universal gas constant and its value is  $8.314 \times 10^{-3}$  kJ/mol-K;  
 $Re$  = Reynolds number;  
 $S_k$  = turbulent kinetic energy source term,  $m^2/s^2$ ;  
 $S_s$  = the mass of the component produced per unit volume per unit time within the system by chemical reaction, i.e. production rate,  $kmol/m^3s$ ;  
 $S_\omega$  = source term defined by users;  
 $t$  = reaction time, s;  
 $T$  = temperature, K;

---

$\bar{T}$	= average temperature, K;
$u$	= velocity of the fluid, m/s;
$u_i$	= velocity of the fluid along with i direction, m/s;
$\bar{u}_i$	= average velocity along with i direction, m/s;
$\bar{u}_j$	= average velocity along with j direction, m/s;
$v$	= inlet velocity, m/s;
$x$	= x-axis;
$x_i$	= x, y;
$x_j$	= x, y;
$y$	= y-axis;
$Y_k, Y_\omega$	= terms representing turbulence generated by diffusion; and
$y^+$	= dimensionless wall distance.

*Greek symbol*

$\Gamma_k$	= diffusion rate of $k$ ;
$\Gamma_\omega$	= diffusion rate of $\omega$ ;
$\lambda$	= thermal conductivity of the fluid, W/m·K;
$\lambda_t$	= turbulent thermal conductivity, W/m·K;
$\mu$	= dynamic viscosity of the fluid, kg/m·s;
$\mu_t$	= turbulent viscosity, kg/m·s;
$\rho$	= density of the fluid, kg/m <sup>3</sup> ;
$\omega$	= specific dissipation; and
$\omega_R$	= the reaction rate, kmol/m <sup>3</sup> ·s.

*Subscripts*

$a$	= average;
$b$	= bulk;
$d$	= downstream section;
$in$	= inlet;
$out$	= outlet;
$pc$	= pseudo-critical temperature;
$t$	= tested section;
$u$	= upstream section; and
$w$	= wall.

*Acronyms*

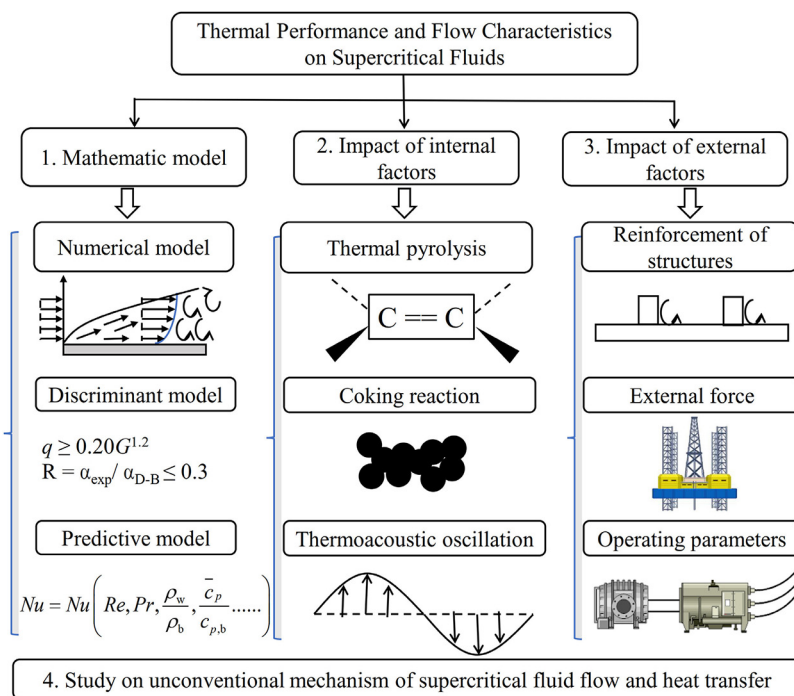
$AKN$	= Abe-Kondoh-Nagano;
$DNS$	= direct numerical simulation;
$HTD$	= heat transfer deterioration;
$HTE$	= heat transfer enhancement;
$LES$	= large eddy simulation;
$LS$	= Launder-Sharma;
$NIST$	= National Institute of Standards and Technology;
$PPD$	= proportional product distribution;
$RANS$	= Reynolds-averaged Navier-Stokes equations;
$RP-3$	= China no. 3 aviation kerosene;
$SST$	= shear stress transport; and
$2-D$	= two-dimensional.

## 1. Introduction

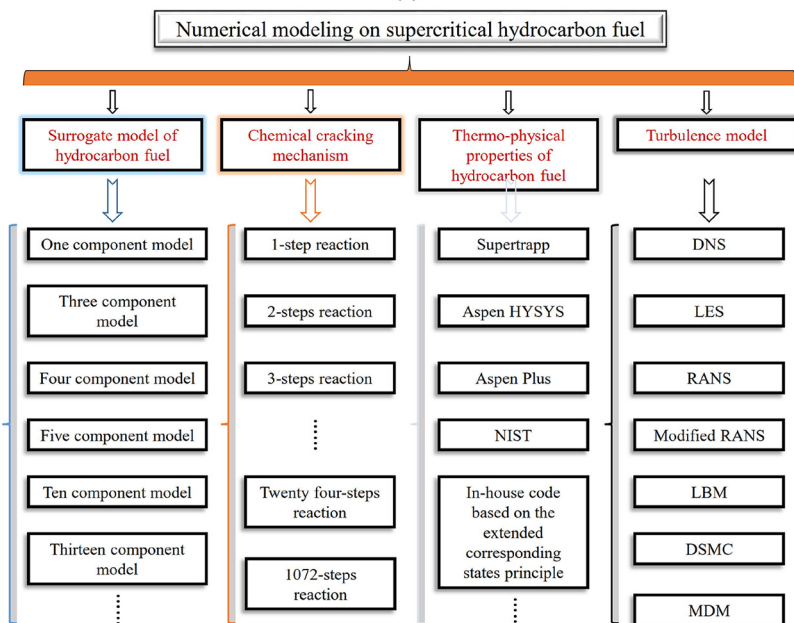
The scramjet engine can provide effective thrust for hypersonic vehicles (Sunden *et al.*, 2016; Li *et al.*, 2021a). However, thermal protection is an extremely crucial issue due to supersonic combustion and aerodynamic heating (Pizzarelli *et al.*, 2016; Daniau *et al.*, 2005). It is widely known that the active regenerative cooling technique [a schematic diagram is provided in Chen *et al.* (2020)] can be used to effectively solve this problem (Rao and Kunzru, 2006; Huang *et al.*, 2002; Tsujikawa and Northam, 1996; Gascoin *et al.*, 2008) and supercritical aviation kerosene is used in such a process. The heat transfer deterioration (HTD) and heat transfer enhancement (HTE) of supercritical hydrocarbon fuels can always be observed (Negoescu *et al.*, 2017; Xie *et al.*, 2021; Kim and Kim, 2010); thus, the relevant heat transfer performance and flow characteristics were paid much attention to. Besides, based on the open published literature, the research in this area is summarized as shown in Figure 1(a), and it focuses on the mathematic model, impact of internal factors, impact of external factors as well as unconventional mechanism of supercritical fluid flow and heat transfer. Regarding the supercritical hydrocarbon fuels, the numerical modelling and operating parameters are described with emphasis in this paper. The numerical models on supercritical hydrocarbon fuels include surrogate model, the chemical cracking mechanism, thermo-physical properties and turbulence models as shown in Figure 1(b).

### 1.1 Surrogate model of hydrocarbon fuels

Aviation kerosene is a compound with complex components, which cannot be thoroughly considered in the computational calculation. Thus, surrogate models of aviation kerosene are extensively used in the literature. Table 1 summarizes the surrogate models of aviation kerosene (Zhang *et al.*, 2017; Fan and Yu, 2006; Ren *et al.*, 2013; Zeng *et al.*, 2014; Xiao *et al.*, 2010; Zheng *et al.*, 2015; Pei and Hou, 2017; Jiang *et al.*, 2013; Cheng *et al.*, 2012; Zhong *et al.*, 2009a; Li *et al.*, 2019a). Apart from literature Jiang *et al.* (2013), the rest are surrogate models of China no. 3 aviation kerosene (RP-3). Specifically, Zhang *et al.* (2017) investigated chemical recuperation in various aspect-ratio channels with n-decane as an alternative of aviation kerosene. In contrast, Fan and Yu (2006) put forward a three-component model, which was verified by an extended corresponding state model. The three-component model was composed of n-decane, trimethylcyclohexane and propylbenzene, which accounted for 0.49, 0.44 and 0.07, respectively, in the mole fraction. Ren *et al.* (2013) also reported a three-component surrogate model that has n-undecane (0.53 mole fraction), 1-butylcyclohexane (0.18 mole fraction) and 1,3,5-trimethyl-benzene (0.29 mole fraction), examined by the RP-3 experiment data. Zeng *et al.* (2014) proposed a three-component surrogate model including 0.65 volume fraction n-decane, 0.1 volume fraction toluene, 0.25 volume fraction propyl cyclohexane. Xiao *et al.* (2010) proposed a reaction model of kerosene using another three-component surrogate model, i.e. n-decane (0.79 mole fraction), trimethylcyclohexane (0.13 mole fraction) and ethylbenzene (0.08 mole fraction). Zheng *et al.* (2015) presented a four-component model, which can accurately evaluate the delayed time of ignition and the speed of laminar flame in real RP-3. The surrogate model includes n-decane, n-dodecane, ethylcyclohexane and xylene, which have a share of 0.4, 0.42, 0.13 and 0.05, respectively in the mole fraction. Pei and Hou (2017) investigated the thermo-physical properties of a four-component surrogate model, which includes n-decane (0.35 mole fraction), n-undecane (0.20 mole fraction), 1-methyl-2-pentyl-cyclohexane (0.40 mole fraction) and 1,3,5-Trimethyl-benzene (0.05 mole fraction) in 300–1000 K and 1–15 MPa. Jiang *et al.* (2013) concluded that the HF-I kerosene can be replaced by a four-component model that has n-decane (0.25 mole



(a)



(b)

**Figure 1.**  
(a) Summary of existing research on supercritical hydrocarbon fuel;  
(b) summary of numerical models of supercritical hydrocarbon fuel

**Table 1.**  
The surrogate  
models of aviation  
kerosene proposed  
by Chinese  
researchers

Substance	Found in	Zhang <i>et al.</i> (2017)	Fan and Yu (2006)	Ren <i>et al.</i> (2013)	Zeng <i>et al.</i> (2014)	Xiao <i>et al.</i> (2010)	Zheng <i>et al.</i> (2015)	Hou (2017)	Pei and Jiang <i>et al.</i> (2013)	Cheng <i>et al.</i> (2012)	Zhong <i>et al.</i> (2009a)	Li <i>et al.</i> (2019a)	
	Amount of components	1 Mole fraction	3 Mole fraction	3 Mole fraction	3 volume fraction	3 Mole fraction	4 Mole fraction	4 Mole fraction	4 Mole fraction	5 Mole fraction	10 Mole fraction	13 Mass fraction	
Alkanes	n-octane (C <sub>8</sub> H <sub>18</sub> )	—	—	—	—	—	—	—	—	—	0.06	0.02188	
	n-nonane (C <sub>9</sub> H <sub>20</sub> )	—	—	—	—	—	—	—	—	—	—	0.06776	
	n-decane (C <sub>10</sub> H <sub>22</sub> )	1	0.49	—	0.65	0.79	0.4	0.35	0.25	0.3886	0.1	0.11623	
	n-undecane (C <sub>11</sub> H <sub>24</sub> )	—	—	0.53	—	—	0.20	—	—	—	—	0.16115	
	n-dodecane (C <sub>12</sub> H <sub>26</sub> )	—	—	—	—	—	0.42	—	0.50	—	0.2	0.1482	
	n-tridecane (C <sub>13</sub> H <sub>28</sub> )	—	—	—	—	—	—	—	0.12	0.2724	0.08	0.10482	
	n-tetradecane (C <sub>14</sub> H <sub>30</sub> )	—	—	—	—	—	—	—	—	—	0.1	0.0535	
	n-pentadecane (C <sub>15</sub> H <sub>32</sub> )	—	—	—	—	—	—	—	—	—	—	0.01862	
	n-hexadecane (C <sub>16</sub> H <sub>34</sub> )	—	—	—	—	—	—	—	—	—	—	—	—
	Cycloalkanes	methylcyclohexane (C <sub>7</sub> H <sub>14</sub> )	—	—	—	—	—	—	—	—	—	0.2	—
trans-1,3- dimethylcyclopentane (C <sub>7</sub> H <sub>14</sub> )		—	—	—	—	—	—	—	—	—	0.08	—	
ethylcyclohexane (C <sub>8</sub> H <sub>16</sub> )		—	—	—	—	—	0.13	—	—	—	—	—	
Propylcyclohexane (C <sub>9</sub> H <sub>18</sub> )		—	—	—	0.25	—	—	—	—	—	—	—	
1,3,5- trimethylcyclohexane (C <sub>9</sub> H <sub>18</sub> )		—	0.44	—	—	0.13	—	—	—	0.0889	—	—	
1,1,4- trimethylcyclohexane (C <sub>9</sub> H <sub>18</sub> )		—	—	—	—	—	—	—	—	—	—	0.06793	
1-decene (C <sub>10</sub> H <sub>20</sub> )		—	—	—	—	—	—	—	—	—	—	0.06543	
(n) 1-butylcyclohexane (C <sub>10</sub> H <sub>20</sub> )		—	—	0.18	—	—	—	—	0.13	0.1111	—	—	
1-methyl-3- isopropylbenzene (C <sub>10</sub> H <sub>14</sub> )		—	—	—	—	—	—	—	—	—	—	—	0.05293
1-methyl-2-pentyl- cyclohexane (C <sub>12</sub> H <sub>24</sub> )		—	—	—	—	—	—	0.40	—	—	—	—	

(continued)

Substance	Found in	Zhang <i>et al.</i> (2017)	Fan and Yu (2006)	Ren <i>et al.</i> (2013)	Zeng <i>et al.</i> (2014)	Xiao <i>et al.</i> (2010)	Zheng <i>et al.</i> (2015)	Hou (2017)	Pei and Jiang <i>et al.</i> (2013)	Cheng <i>et al.</i> (2012)	Zhong <i>et al.</i> (2009a)	Li <i>et al.</i> (2019a)
Benzenes	toluene (C <sub>7</sub> H <sub>8</sub> )	-	-	-	0.1	-	-	-	-	-	-	-
	ethylbenzene (C <sub>8</sub> H <sub>10</sub> )	-	-	-	-	0.08	-	-	-	-	-	-
	p-xylene (C <sub>8</sub> H <sub>10</sub> )	-	-	-	-	-	0.05	-	-	-	-	-
	n-Propylbenzene (C <sub>9</sub> H <sub>12</sub> )	-	0.07	-	-	-	-	-	-	0.139	0.05	-
	1,3,5-Trimethyl-benzene (C <sub>9</sub> H <sub>12</sub> )	-	-	0.29	-	-	-	0.05	-	-	-	0.09454
	1-methylnaphthalene (C <sub>11</sub> H <sub>10</sub> )	-	-	-	-	-	-	-	-	-	0.03	0.0471

Table 1.

fraction), n-dodecane (0.50 mole fraction), n-tridecane (0.12 mole fraction) and n-butylcyclohexane (0.13 mole fraction). Additionally, many other surrogate models of RP-3 have been reported as shown in Table 1 (Cheng *et al.*, 2012; Zhong *et al.*, 2009a; Li *et al.*, 2019a).

### 1.2 Chemical cracking mechanism of hydrocarbon fuels

It is widely known that the cracking reaction can be observed once the temperature is above 750 K (Edwards, 2006). The endothermic pyrolysis essentially affects supercritical thermal transport. Thus, it is critical to reveal the chemical cracking mechanism of hydrocarbon fuels. Based on the literature, the detailed reaction mechanism, lumped reaction mechanism and global reaction mechanism are commonly used as the cracking reaction models of supercritical hydrocarbon fuels. Furthermore, these cracking reaction models are embedded in commercial softwares such as ANSYS FLUENT, and this procedure is used to study the coupling of the cracking reaction, flow characteristics and heat transfer behavior. Ward *et al.* (2004, 2005) proposed two chemical cracking mechanisms of one-step proportional product distribution (PPD), and these models were used by Bao *et al.* (2014), Zhao *et al.* (2018), Tao *et al.* (2018a), Lei *et al.* (2020) and Sun *et al.* (2018a). Dahm *et al.* (2004) suggested 1175 reactions and 175 species of n-dodecane using the EXGAS software. Herbinet *et al.* (2007) also used the EXGAS software to report 1449 reactions and 271 species of n-dodecane. Xing *et al.* (2009) and Zhong *et al.* (2009b) studied the kinetic parameters of global reaction of RP-3 at  $p = 2.0\text{--}3.9\text{ MPa}$ ,  $T = 663\text{--}703\text{ K}$  and  $p = 3.5\text{--}4.5\text{ MPa}$ ,  $T = 700\text{--}1100\text{ K}$ . Jiang *et al.* (2013) presented a molecular reaction model with 28 species and 24 reactions, and the computational accuracy was acceptable when the cracking conversion was less than 86%. Furthermore, this chemical cracking mechanism was adopted by Zhao *et al.* (2015), Zhang *et al.* (2015), Xu and Meng (2015a) and Jing *et al.* (2018) to study the impact of pressure on the fuel cracking, thermo-hydrodynamic characteristics and curved regenerative cooling channels, respectively. Hou *et al.* (2013) established a global reaction of one-step thermal cracking based on the proportional product distributions and gaseous-product experiments. Ruan *et al.* (2014) developed a reduced 12-species chemical cracking mechanism, and it was also applied to analyze the effects of the endothermic fuel cracking on thermo-hydrodynamic characteristics (Sun *et al.*, 2018b). Zhu *et al.* (2014) gave a global reaction framework including 18 species in conditions of  $p = 4.2\text{--}5.3\text{ MPa}$ , and  $T = 860\text{--}910\text{ K}$ . Zhou *et al.* (2017) created a one-step global mild-cracking reaction framework for n-decane with 11 species. Wang *et al.* (2017) obtained a small-scale chemical reaction model of n-decane in conditions of 4 MPa, 480–720°C. Jiao *et al.* (2018) reported a molecular kinetic model with 15-steps reactions and only one primary reaction is included. Li *et al.* (2019b) proposed a simplified chemical cracking mechanism with 16 species and 11 reactions. The chemical cracking mechanisms mentioned above are summarized in Table 2.

### 1.3 Thermo-physical properties of hydrocarbon fuels

It is vital to obtain accurate properties of aviation kerosene for computational calculation. According to the existing literature, SUPERTRAPP, Aspen HYSYS, Aspen Plus and REFPROP, developed by the National Institute of Standards and Technology (NIST) (NIST, 1999), are always used to achieve the properties of aviation kerosene (Yang *et al.*, 2020; Li *et al.*, 2018; Bao *et al.*, 2012; Jiao *et al.*, 2020). The properties are also obtained by in-house codes based on extended corresponding state principles, which are always incorporated into the commercial softwares (Ruan *et al.*, 2014; Tao *et al.*, 2019; Wang *et al.*, 2010). Besides, the Chemkin files (CHEMKIN-PRO 15092, 2009) can be imported into the ANSYS FLUENT to build the reaction model (Zhou *et al.*, 2017). Herein, two things need to be confirmed. First,

Authors (Year)	Reaction steps	Chemical cracking reactions	Measurement conditions	Activation energy	
				$E_a$ kcal/mol (kJ/mol)	A factor A, s <sup>-1</sup> (%) conversion
Ward <i>et al.</i> (2004)	1-step (19-species)	$C_{10}H_{22} \rightarrow 0.151 H_2 + 0.143 CH_4 + 0.256 C_3H_4 + 0.126 C_2H_6 + 0.230 C_3H_6 + 0.180 C_3H_8 + 0.196 C_3H_8 + 0.102 C_4H_{10} + 0.171 C_5H_{10} + 0.124 C_5H_{12} + 0.195 C_6H_{12} + 0.089 C_6H_{14} + 0.169 C_7H_{14} + 0.072 C_7H_{16} + 0.152 C_8H_{16} + 0.012 C_8H_{18} + 0.053 C_9H_{18} + 0.003 C_9H_{20}$	$p = 3.45 \text{ MPa}$ , $T = 773\text{--}873 \text{ K}$ .	63 (263.34)	$2.1 \times 10^{15}$ < 20%
Adopted by others Ward <i>et al.</i> (2005)	1-step (18-species)	$C_{10}H_{22} \rightarrow 0.153 CH_4 + 0.222 C_2H_4 + 0.138 C_2H_6 + 0.2 C_3H_6 + 0.185 C_3H_8 + 0.171 C_4H_8 + 0.118 C_4H_{10} + 0.149 C_5H_{10} + 0.137 C_5H_{12} + 0.17 C_6H_{12} + 0.106 C_6H_{14} + 0.147 C_7H_{14} + 0.091 C_7H_{16} + 0.132 C_8H_{16} + 0.04 C_8H_{18} + 0.046 C_9H_{18} + 0.031 C_9H_{20}$	$p = 3.45$ – 11.38 MPa, $T = 823\text{--}873 \text{ K}$ .	63 (263.34)	$1.6 \times 10^{15}$ < 35%
Adopted by others Dahm <i>et al.</i> (2004)	Sum <i>et al.</i> (2018a) 1175-steps (175-species)	1175 reactions of n-dodecane using EXGAS software, it is difficult to couple detailed kinetic models with CFD code	$p = 0.1 \text{ MPa}$ , $T = 950, 1000,$ 1050 K.	–	–
Adopted by others Herbinet <i>et al.</i> (2007)	None 1449-steps (271-species)	1449 reactions of n-dodecane using EXGAS software, it is difficult to couple detailed kinetic models with CFD code	$p = 0.1 \text{ MPa}$ , $T = 500\text{--}1500 \text{ K}$ .	–	–
Adopted by others Xing <i>et al.</i> (2009)	None 1-step	–	$p = 2.0\text{--}3.9 \text{ MPa}$ , $T = 663\text{--}703 \text{ K}$ .	66.99 (280 ± 6.5)	$\log A = 19.3 \pm 0.5$
Adopted by others Zhong <i>et al.</i> (2009b)	None 1-step (18-species)	–	$p = 3.5\text{--}4.5 \text{ MPa}$ , $T = 700\text{--}1100 \text{ K}$ .	67.5 (282.15)	$7.2 \times 10^{10}$
Adopted by others Jiang <i>et al.</i> (2013)	None 24-steps (18-species)	Primary reaction: $HF-I (C_{11}, ssH_{23}, s_2) \rightarrow 0.1086 H_2 + 0.4773 CH_4 + 0.5586 C_2H_4 + 0.39 C_2H_6 + 0.41 C_3H_6 + 0.2001 C_3H_8 +$	$p = 5 \text{ MPa}$ , $T = 953\text{--}973 \text{ K}$ .	52.13 (217.9)	$2.869 \times 10^{14}$ < 86%

(continued)

Supercritical  
aviation  
kerosene

3047

**Table 2.**  
The kinds of  
chemical cracking  
reactions of aviation  
kerosene proposed  
based on present  
literature

Authors (Year)	Reaction steps	Chemical cracking reactions	Measurement conditions	Activation energy $E_a$ , kcal/mol (kJ/mol)	A factor $A$ , s <sup>-1</sup>	(%) conversion
<i>Adopted by others</i> <a href="#">Hou et al. (2013)</a>	1-step (9-species)	$0.2246 C_4H_8 + 0.0353 C_7H_{10} + 0.031 C_4H_6 + 0.7201 C_{5+} + 0.27 C_{C_{5+}} + 0.0222 C_nH_{2n-6}$ $C_{12}H_{23} \rightarrow 0.16 H_2 + CH_4 + 0.58 C_2H_6 + 0.43 C_2H_4 + 0.42 C_3H_6 + 0.28 C_3H_8 + 0.25 C_4H_8 + 0.84 C_4H_8$	$p = 1-3 \text{ MPa}$ $T = 780-988 \text{ K}$	63 (263.34)	$2.1 \times 10^{15}$	-
<i>Adopted by others</i> <a href="#">Ruan et al. (2014)</a>	None 1-step (12-species)	$C_{10}H_{22} \rightarrow 0.153 CH_4 + 0.222 C_2H_4 + 0.138 C_2H_6 + 0.200 C_3H_6 + 0.185 C_3H_8 + 0.171 C_4H_8 + 0.118 C_4H_{10} + 0.149 C_5H_{10} + 0.137 C_5H_{12} + 0.630 C_6H_{12} + 0.268 C_6H_{14}$	-	63 (263.34)	$1.6 \times 10^{15}$	-
<i>Adopted by others</i> <a href="#">Zhu et al. (2014)</a>	1-step (18-species)	$C_{10}H_{22} \rightarrow 0.0170 H_2 + 0.1827 CH_4 + 0.1980 C_2H_4 + 0.1327 C_2H_6 + 0.0566 C_3H_6 + 0.0372 C_3H_8 + 0.0135 C_4H_8 + 0.0048 C_4H_{10} + 0.2015 C_5H_{10} + 0.1167 C_5H_{12} + 0.3033 C_6H_{12} + 0.0735 C_6H_{14} + 0.2611 C_7H_{14} + 0.0684 C_7H_{16} + 0.2209 C_8H_{16} + 0.0130 C_8H_{18} + 0.0817 C_9H_{18} + 0.0040 C_9H_{20}$	$p = 4.2-5.3 \text{ MPa}$ $T = 860-910 \text{ K}$	63 (263.34)	$1.6 \times 10^{15}$	< 13%
<i>Adopted by others</i> <a href="#">Zhou et al. (2017)</a>	None 1-step (11-species)	$C_{10}H_{22} \rightarrow 0.31 CH_4 + 0.46 C_2H_6 + 0.89 C_2H_4 + 0.17 C_3H_8 + 0.37 C_3H_6 + 0.05 C_4H_{10} + 0.09 C_4H_8 + 0.04 C_4H_6 + 0.07 H_2 + 0.77 C_{5+}$	$p = 3.5-4.0 \text{ MPa}$ $T = 880-890 \text{ K}$	64.3 (268.774)	$1.75 \times 10^{15}$	< 12%
<i>Adopted by others</i> <a href="#">Wang et al. (2017)</a>	None 22-steps (16-species)	$C_{10}H_{22} \rightarrow 0.044 H_2 + 0.186 CH_4 + 0.321 C_2H_4 + 0.286 C_2H_6 + 0.212 C_3H_6 + 0.166 C_3H_8 + 0.040 C_4H_8 + 0.026 C_4H_{10} + 0.004 C_4H_6 + 0.813 C_{5+} + 0.001 C_nH_{2n-6}$	$p = 4.0 \text{ MPa}$ $T = 753-993 \text{ K}$	59.4 (248.292)	$6.209 \times 10^{15}$	< 93%

(continued)

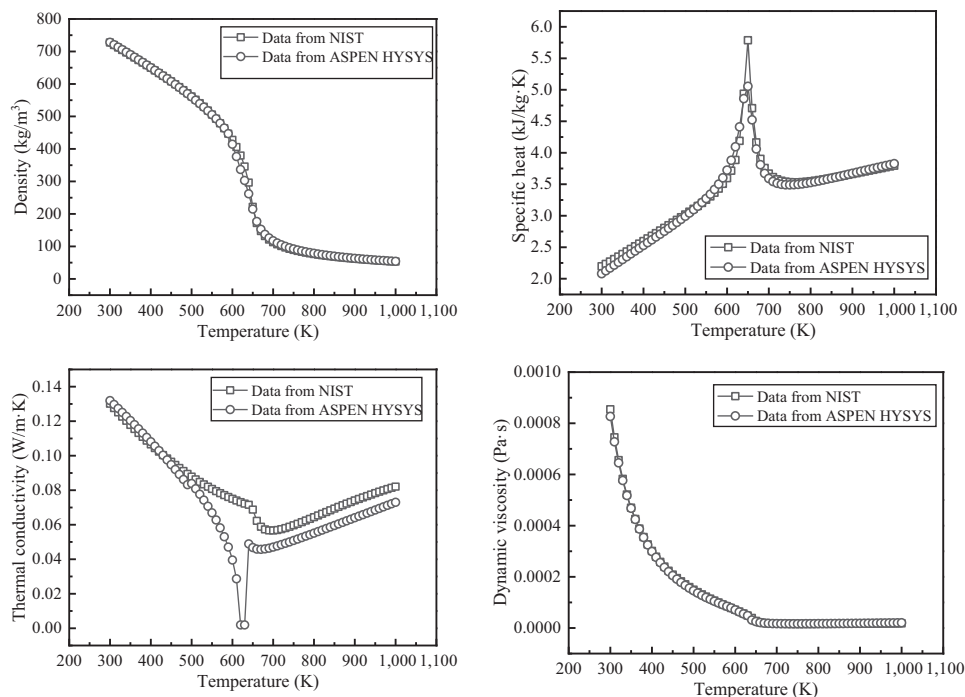
Authors (Year)	Reaction steps	Chemical cracking reactions	Measurement conditions	Activation energy $E_a$ , kcal/mol (kJ/mol)	A factor A, s <sup>-1</sup>	(%) conversion
<i>Adapted by others</i> Jiao <i>et al.</i> (Jiao <i>et al.</i> , 2018) (2018)	None 15-steps (12-species)	<i>Primary reaction:</i> $C_{10}H_{22} \rightarrow 0.01047 H_2 + 0.20441 CH_4 + 0.33964 C_2H_6 + 0.5222 C_2H_4 + 0.2752 C_3H_8 + 0.3722 C_3H_6 + 0.13114 C_4H_{10} + 0.39672 C_4H_8 + 0.62688 C_{4+}$	$p = 3\text{--}5\text{ MPa}$ , $T = 943.15\text{--}923.52\text{ K}$ .	58.54 (244.71)	3 MPa: $4.52 \times 10^{15}$ , 4 MPa: $5.22 \times 10^{15}$ , 5 MPa: $5.69 \times 10^{15}$	< 15%
<i>Adapted by others</i> Li <i>et al.</i> (2019b)	None 11-steps (16-species)	<i>Primary reaction:</i> $HF-I (C_{11,ss}H_{23,82}) \rightarrow 0.07386 H_2 + 0.4710 CH_4 + 0.2981 C_2H_4 + 0.4174 C_2H_6 + 0.3287 C_3H_6 + 0.2483 C_3H_8 + 0.3007 C_4H_8 + 0.1646 C_4H_{10} + 0.0331 C_4H_6 + 0.6411 C_5 + 0.243 CC_5 + 0.05308 C_{4+}H_{2n+6}$	$p = 3.5\text{ MPa}$ , $T = 798\text{--}973\text{ K}$ .	56.6 (236.6)	$1.223 \times 10^{14}$	< 70%
<i>Adapted by others</i>	None					

Table 2.

the thermo-physical properties of the same substance calculated by different softwares must be consistent. Second, the thermo-physical properties of the different surrogate models of hydrocarbon fuels calculated by the same software must be consistent.

To start, n-decane is selected as the object of comparison. Its thermo-physical properties calculated by REFPROP and ASPEN HYSYS are compared and shown in Figure 2. It is obvious that the two softwares give similar density and dynamic viscosity. Besides, their specific heats are similar except for the maximum value. However, an obvious difference can be observed regarding the thermal conductivity. Thus, it should be careful to use the thermal properties of supercritical fluids, which need to be validated by the experimental data.

Then, the thermo-physical properties of the different surrogate models of hydrocarbon fuels calculated by the same software should be compared before the numerical simulations. Fortunately, this work has been partially done by Xu and Meng (2015b). The thermodynamic and transport properties of five surrogate models of RP-3 were examined including one-species, three-species in Fan et al. (2006), four-species in Mawid et al. (2003), six-species in Lenhart et al. (2007) and ten-species in Zhong et al. (2009a). It was found that the four-species model showed an excellent performance with experimental data, and it was regarded as the most preferable option. Surprisingly, the one-species model, saying n-decane, also showed an appropriate performance. Besides, Cheng et al. (2016) evaluated the three-species (Ren et al., 2013), three-species (Fan and Yu, 2006), four-species (Dagaut and Cathonnet, 2006), six-species (Violi et al., 2002), ten-species (Zhong et al., 2009a), and it was indicated that the surrogate model of three-species in Ren et al. (2013) can predict the thermo-physical properties well. In this work, the surrogate models of one-species in Zhang et al. (2017), three-species in Xiao et al. (2010), four-species in Jiang et al. (2013), five-species in Cheng et al. (2012) and ten-species in Zhong et al. (2009a) listed in Table 1 are carefully examined and the thermo-



**Figure 2.** Thermo-physical properties of n-decane along with the temperature under the conditions of  $p = 3.0 \text{ MPa}$

physical properties of these models calculated by the ASPEN HYSYS are compared with the experimental data in [Deng \*et al.\* \(2011, 2012a, 2012b\)](#). This is because some important components cannot be found in NIST. As shown in [Figures 3–7](#), for all the surrogate models of the hydrocarbon fuel, the calculated density and dynamic viscosity are consistent with the experimental data in [Deng \*et al.\* \(2011, 2012a, 2012b\)](#). However, for the specific heat, a large difference is found among different surrogate models, particularly in the supercritical-temperature region. Especially, the value of the supercritical temperature for the four-species surrogate model matches well with the experimental data due to the same position of the maximum specific heat. It is concluded that the usage of the properties of the hydrocarbon fuel should be carefully done and those data also should be validated by the experimental data as long as possible.

#### 1.4 Turbulence models

The numerical methods such as Direct Numerical Simulation (DNS), Large Eddy Simulation (LES) and Reynolds-averaged Navier Stokes (RANS) with wall treatment have been assessed ([Li \*et al.\*, 2014](#); [Bae and Yoo, 2005](#); [Niceno and Sharabi, 2013](#);

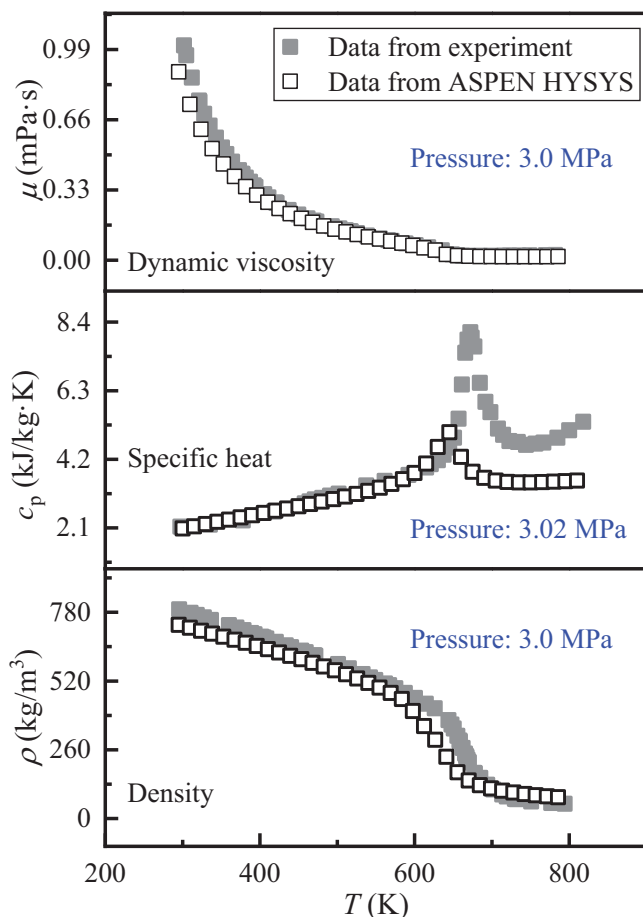


**Figure 3.** Comparison between the data from the experiment ([Deng \*et al.\*, 2011](#); [Deng \*et al.\*, 2012a](#); [Deng \*et al.\*, 2012b](#)) and data from ASPEN HYSYS for one-species surrogate model in [Zhang \*et al.\* \(2017\)](#)

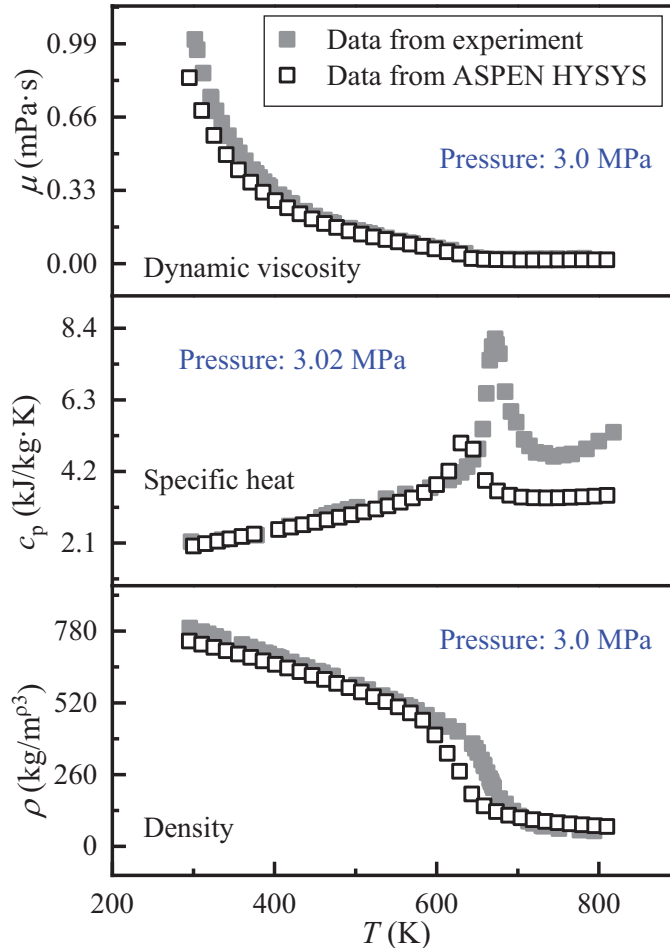


**Figure 4.** Comparison between the data from experiment (Deng *et al.*, 2011; Deng *et al.*, 2012a; Deng *et al.*, 2012b) and data from ASPEN HYSYS for three-species surrogate model in Xiao *et al.* (2010)

Wen and Gu, 2010; Xu *et al.*, 2018a). Among them, the RANS is paid much attention because the current turbulence models in RANS are built based on constant physical properties at subcritical conditions (Li *et al.*, 2014), so that they cannot correctly predict the supercritical heat transfer behavior due to the extremely dramatical thermo-physical properties. Therefore, the modifications of the turbulence models in RANS are intensively studied. Tao *et al.* (2018b) modified the LS (Launder–Sharma) low-Reynolds number turbulence model based on the density fluctuation. Li *et al.* (2016) improved the prediction accuracy of HTD by considering the density fluctuation and thermal expansion coefficient fluctuation in the AKN turbulence model (Abe *et al.*, 1994). Jiang *et al.* (2018) considered the buoyancy-induced production of turbulent kinetic energy and the turbulent Prandtl number to improve the prediction ability of the HTD.

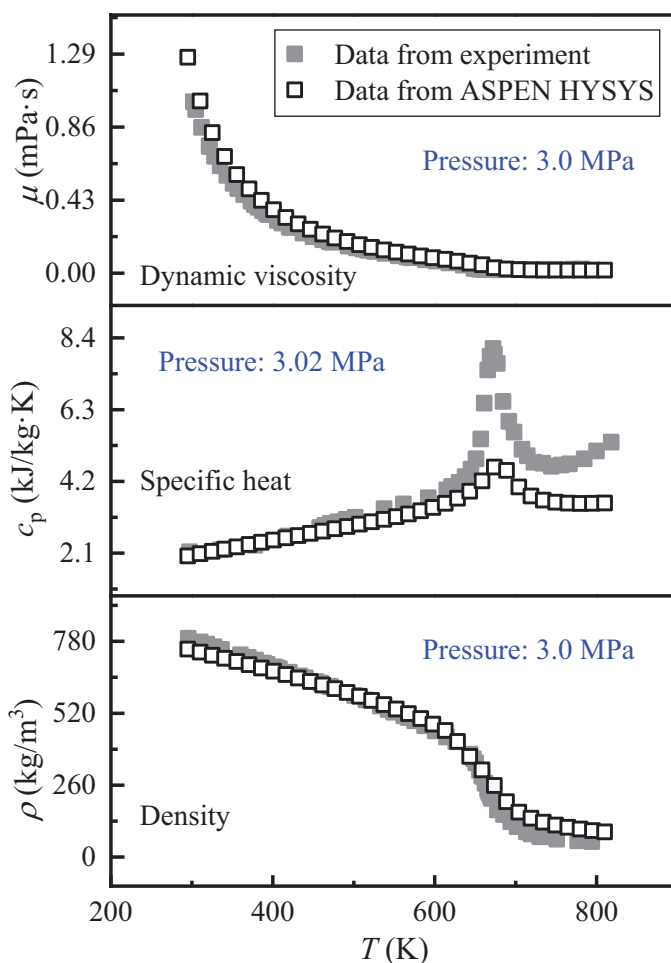


**Figure 5.** Comparison between the data from experiment (Deng *et al.*, 2011; Deng *et al.*, 2012a; Deng *et al.*, 2012b) and data from ASPEN HYSYS for four-species surrogate model in Jiang *et al.* (2013)

### 1.5 Flow characteristics and thermal performances

As the above-related issues are resolved, the flow characteristics and thermal performances of supercritical hydrocarbon fuels can be investigated. The experimental research and numerical research are described, respectively.

*Experimental research:* Zhong *et al.* (2009a) analytically derived heat transfer coefficients of a 10-species surrogate model in extensive temperature, pressure, and flow rate of 300–1000 K, 2.6–5.0 MPa, and 10–100 g/s, respectively. It was reported that the HTE phenomenon occurs once the supercritical condition appears. Zhang *et al.* (2012) studied thermal transport of hydrocarbon fuel in an upward-flowing tube, indicating that the HTD phenomenon appeared once the acceleration parameter ( $Kv$ ) was smaller than  $1.5 \times 10^{-8}$  or the buoyancy factor ( $Bo^*$ ) was lower than  $1.6 \times 10^{-10}$ . Zhu *et al.* (2013) concentrated on the flow resistance of hydrocarbon fuel in a round tube placed horizontally with varied pressure, temperature and flow rates. It was concluded that high temperature and flow rates

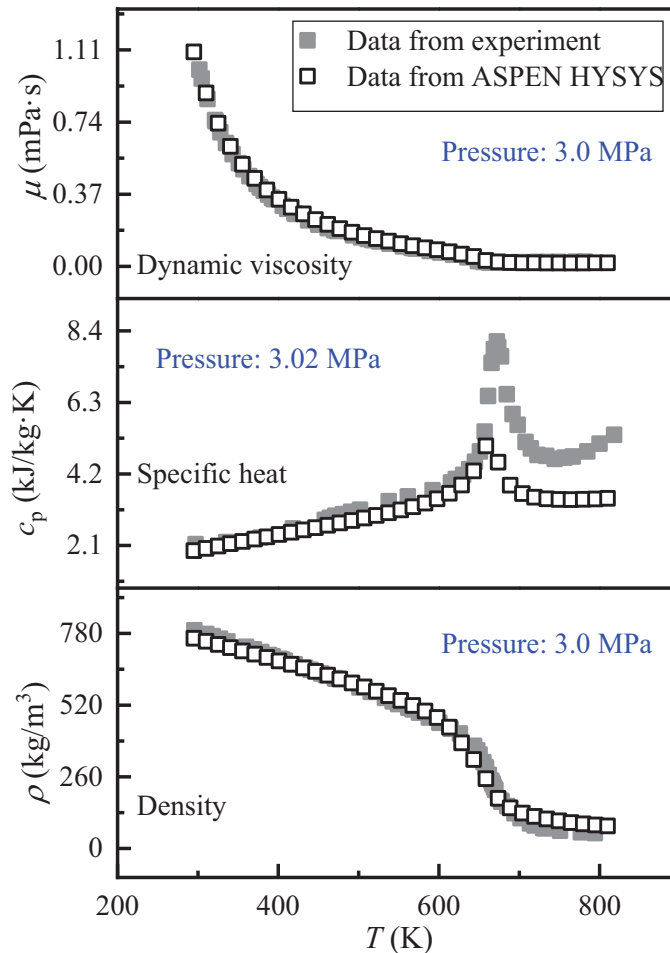


**Figure 6.** Comparison between the data from experiment (Deng *et al.*, 2011; Deng *et al.*, 2012a; Deng *et al.*, 2012b) and data from ASPEN HYSYS for five-species surrogate model in Cheng *et al.* (2012)

corresponded to large pressure drops. Fu *et al.* (2017a, 2017b) analyzed the convective heat transfer in vertical and U-turn tubes with various pressure, heating conditions, flow rates and tube sizes, finding that the heat transfer intensity agreed well with the existing correlation when  $T_b/T_{pc} < 0.80$  and the heat transfer intensity increased with the decreasing diameter of the bend. Huang *et al.* (2015) also studied the effect of the key parameters on the thermal transport of supercritical fuel. Wen *et al.* (2017a) addressed the effect of buoyancy force on supercritical thermal transport, which could be evaluated by the  $Gr_q/Gr_{th}$  (Petukhov *et al.*, 1974). They also studied supercritical fuel in a vertical helical pipe, which presented that the heat transfer intensity of the outside was 31.5% larger than that of the inside due to the centrifugal secondary flow (Wen *et al.*, 2017b). Jia *et al.* (2019) explored the effect of an initiator (nitropropane) on the hydrocarbon pyrolysis in a miniature pipe, and it was demonstrated that the pyrolysis temperature of n-decane was reduced by 100 K. Qin *et al.* (2013) clarified the parameter-dependent chemical recuperation process of supercritical hydrocarbon fuel. Liang *et al.* (2017) researched the impact of high pyrolysis on thermal

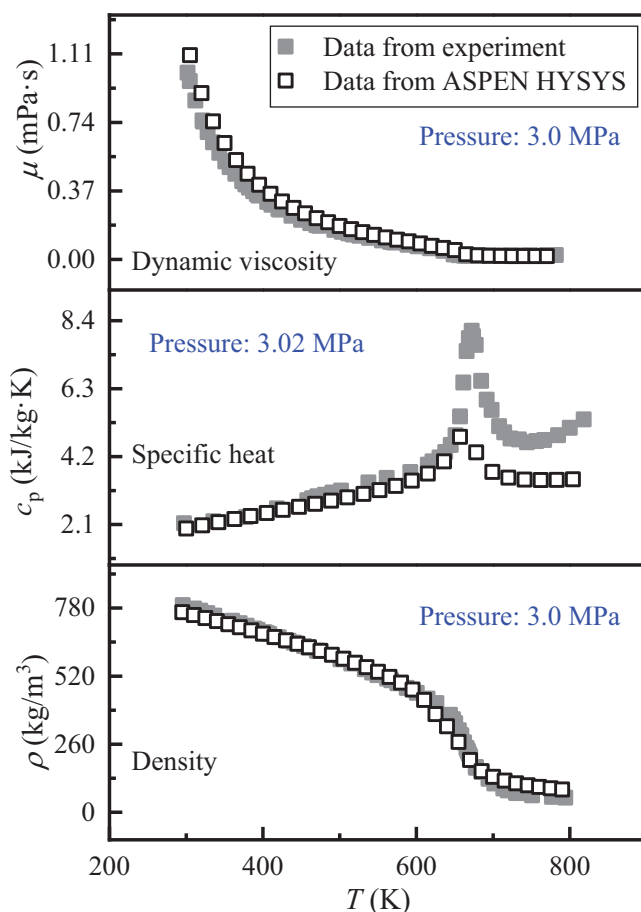


**Figure 7.** Comparison between the data from experiment (Deng *et al.*, 2011; Deng *et al.*, 2012a; Deng *et al.*, 2012b) and data from ASPEN HYSYS for 10-species surrogate model in Zhong *et al.* (2009a)

performance and a critical heat flux of 0.4–0.5 MW/m<sup>2</sup> was confirmed. Liu *et al.* (2019a) innovatively proposed an online hybrid method to analyze the pyrolysis mechanism. Wang *et al.* (2019) introduced the formation mechanisms of thermo-acoustic instability in a vertical upward circular tube. Jiang *et al.* (2019) announced that an additional heat sink will be activated once thermal cracking happens. Liu *et al.* (2019b) compared the thermo-hydrodynamic characteristics at the conditions of asymmetric heating and uniform heating.

Most of the above studies focused on the flow characteristics and thermal performances of supercritical aviation kerosene as well as the cracking reactions. The influence mechanism of convective heat transfer with pyrolysis reaction is difficult to explain by experimental data. Thus, numerical simulations are required to use the impact of the cracking reaction on the thermal transport.

*Numerical research:* Many studies were numerically implemented to study the thermal transport of supercritical fuel but the cracking reaction was not fully considered (Li *et al.*, 2019c; Li *et al.*, 2020; Cheng *et al.*, 2018; Pu *et al.*, 2019). Fortunately, the cracking reaction was considered in some openly published literature. Hu *et al.* (2017) pointed out that the

pressure drop could be increased due to the thermal-induced acceleration caused by the cracking reaction. [Gong et al. \(2019\)](#) studied the secondary reaction in the thermal transport of supercritical fuel. It was evidenced that the HTD phenomenon could be reduced by the secondary exothermic reaction. [Xu and Meng \(2016\)](#), [Xu et al. \(2018b\)](#) examined the convective heat transfer as well as the cracking reaction and surface coking in a round pipe and a ribbed pipe for supercritical fuel. It was reported that heat transfer was improved by the extra heat sink because of the thermal cracking and thermal-induced acceleration. Also, the pyrolytic chemical reaction rate was increased and the pyrolytic surface coking was decreased due to the effect of the ribs.

Thermal pyrolysis has been considered in the thermal transport of supercritical fuel, as discussed above, but which mostly focused on operating conditions, e.g. pressure, inlet temperature, flow orientation, pipe size and heat/mass flux ratio. The real impacts of the thermal pyrolysis on thermo-hydrodynamic characteristics of supercritical fuel are, however, not completely revealed until now. Therefore, further studies should be executed to clarify the underlying mechanism. In this work, only one operating condition is chosen to detect the impact of thermal pyrolysis on thermal transport in a horizontal tube (the upper wall cooling duct of the combustion chamber) and the typical conditions are  $p = 3.0$  MPa,  $T_{in} = 500$  K,  $v_{in} = 0.7$  m/s ( $q_m = 1.5$  g/s),  $q_w = 1.5$  MW/m<sup>2</sup> (only one wall is heated),  $a = 2$  mm (the size of a rectangular channel).

## 2. Computational domain

A detailed description of the numerical model has been illustrated in [Li et al. \(2021b\)](#), as also shown in [Figure 8](#). Rectangular channels are normally used to wrap combustion chambers to cool the combustor wall. When a hypersonic vehicle is flying horizontally, the cooling channels near the upper and lower wall are different because of the influence of gravity. In this study, the cooling channel near the upper wall serves as the object of the study. Only one channel is considered in the convective heat transfer with thermal pyrolysis in terms of symmetry. Furthermore, a two-dimensional (2-D) computational domain is applied due to the huge computational complexity of thermal pyrolysis. The entire computational domain is divided into three parts: a 30 mm upstream section to guarantee that the turbulence is fully developed, a 100 mm test section to obtain the data of interest, a 30 mm downstream section to prevent the backflow. The inlet size of the cooling channel is selected as 2 mm. The horizontal flow is analyzed in the study and the gravity is strictly involved because of the importance of the buoyancy force ([Wen et al., 2017a](#)).

## 3. Numerical procedure

### 3.1 Governing equations

The fluid flow and heat transfer processes in a horizontal tube are governed by the mass/momentum/energy conservation equations. Also, the thermal pyrolysis is solved by the species mass conservation equation. These formulas are given below.

$$\frac{\partial(\rho \bar{u}_i)}{\partial x_i} = 0 \quad (1)$$

$$\frac{\partial}{\partial x_j}(\rho \bar{u}_i \bar{u}_j) = -\frac{\partial \bar{p}}{\partial x_i} + \frac{\partial}{\partial x_j} \left[ \mu \frac{\partial \bar{u}_i}{\partial x_j} - \rho \overline{u'_i u'_j} \right] + \rho g_i \quad (2)$$

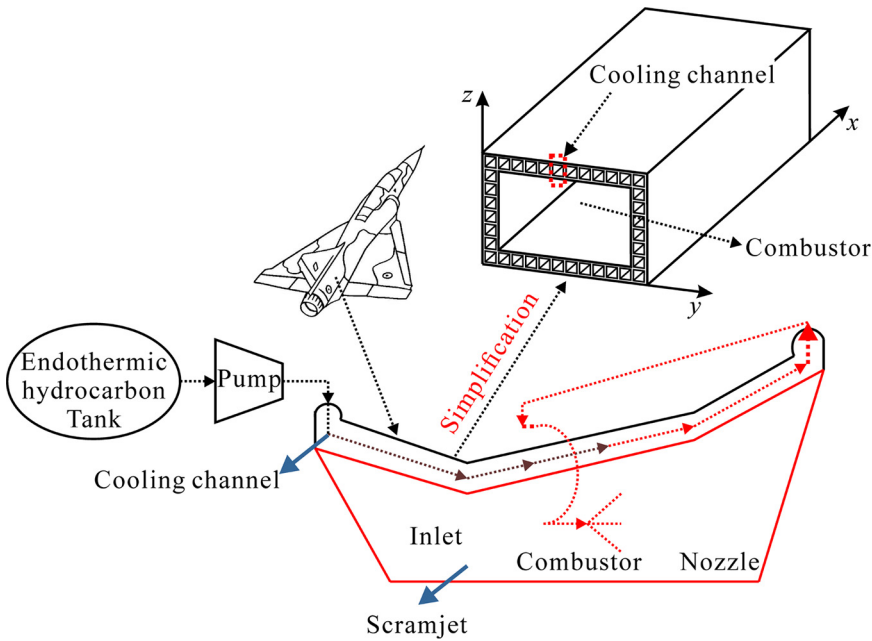


**Figure 8.** Schematic of a scramjet engine with a regenerative cooling system: the endothermic hydrocarbon fuel is heated in the cooling channels and then injected into the combustor

$$\frac{\partial}{\partial x_i} (\rho \bar{u}_i \bar{T}) = \frac{\partial}{\partial x_i} \left[ \left( \frac{\lambda}{c_p} + \frac{\mu_t}{Pr_t} \right) \frac{\partial \bar{T}}{\partial x_i} \right] \quad (3)$$

$$Pr_t = \frac{\mu_t c_p}{\lambda_t} \quad (4)$$

$$\frac{\partial}{\partial x_i} (\rho u_i c_s) = \frac{\partial}{\partial x_i} \left( D_s \frac{\partial \rho c_s}{\partial x_i} \right) + S_s \quad (5)$$

Based on the open published literature (Zhao *et al.*, 2017; Han *et al.*, 2018) and validation described in Section 4, the SST  $k-\omega$  is requisitioned, and the corresponding formulas are supplied below:

$$\frac{\partial(\rho k)}{\partial t} + \frac{\partial(\rho u_i k)}{\partial x_i} = \frac{\partial}{\partial x_i} \left[ (\mu + \sigma_k \mu_t) \frac{\partial k}{\partial x_i} \right] + G_k - Y_k + S_k \quad (6)$$

$$\frac{\partial(\rho \omega)}{\partial t} + \frac{\partial(\rho u_i \omega)}{\partial x_i} = \frac{\partial}{\partial x_j} \left[ \Gamma_\omega \frac{\partial \omega}{\partial x_j} \right] + G_\omega - Y_\omega + D_\omega + S_\omega \quad (7)$$

3.2 Boundary conditions

The initial and boundary conditions are important for solving the governing equations, which are shown in Figure 9. Specifically, On the inlet of the channel, an inlet temperature and a mass flow rate are designated to be 500 K and 1.5 g/s ( $v_{in} = 0.7$  m/s), respectively, while the operating pressure is 3.0 MPa. The boundary condition of outflow is used on the outlet of the channel. A heat flux of 1.5 MW/m<sup>2</sup> is applied to a single wall, while the other walls are set as adiabatic. Noting that the solid zone in this work is not considered. Only the flow characteristic and heat transfer in fluid zone are paid attention under the condition of single wall heating, i.e. nonuniform heating. This type of heating exists in the practical application.

3.3 Chemical kinetics model

As stated in Section 1.2, a large amount of chemical cracking mechanisms of hydrocarbon fuels are provided in previous studies. The PPD chemical cracking mechanism put forward by Ward *et al.* (2004) has been applied by many researchers. In this study, this chemical cracking model is also adopted and its expression is shown as follows:

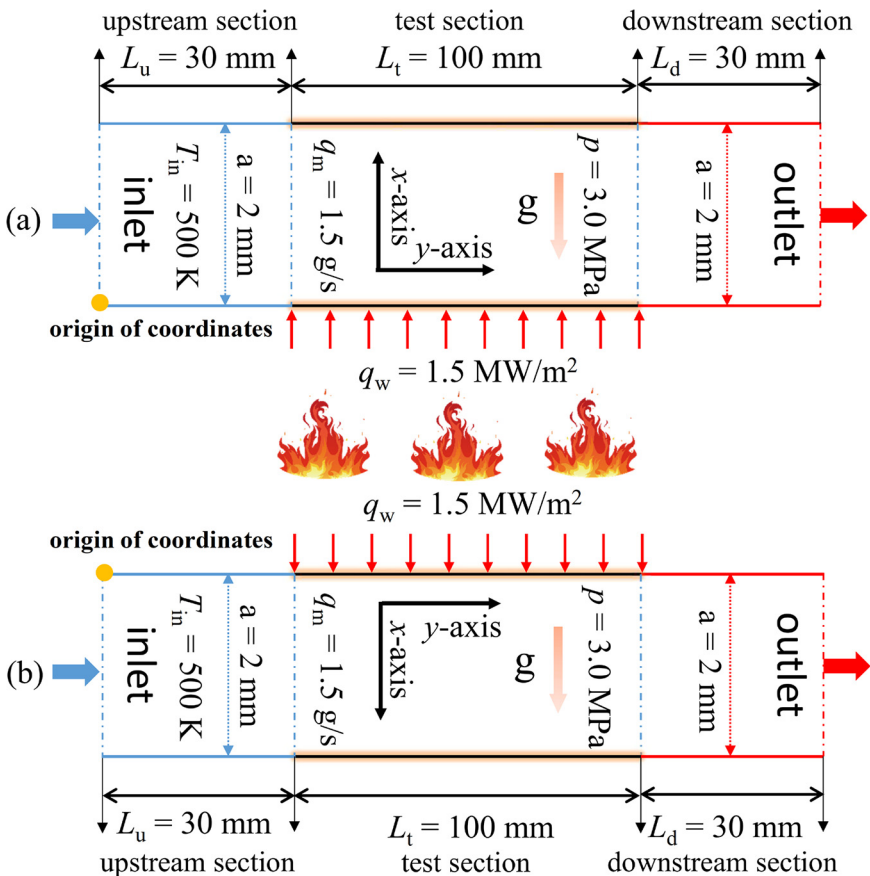
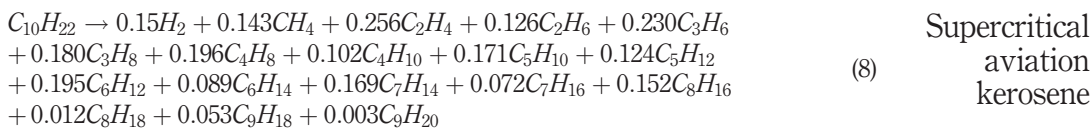


**Figure 9.** Computational domain to study the effects of thermal pyrolysis on the convective heat transfer, and it is divided into three parts: upstream section, test section and downstream section: (a) the upper wall cooling channel of the combustion chamber; (b) the lower wall cooling channel of the combustion chamber



Supercritical  
aviation  
kerosene

The reaction rate of the thermal pyrolysis of supercritical n-decane can be written as:

$$\omega_R = dC_R/dt = -KC_R \tag{9}$$

$$K = k_0 \cdot \exp\left(-\frac{E_a}{RT}\right) \tag{10}$$

**3059**

where  $k_0$  is pre-exponential factor and its value is  $1.6 \times 10^{15}$  1/s,  $E_a$  is activation energy and its value is 263.34 kJ/mol.

### 3.4 Thermo-physical properties

At present, n-decane is used as the surrogate model of aviation kerosene. The thermo-physical properties of reactant and pyrolysis products were calculated by the ASPEN HYSYS. Then, as for the mixture, the specific heat, the density and the thermal conductivity and viscosity were deduced by the volume-weighted mixing law, the mixing law and the mass-weighted mixing law, respectively. These mixing laws can be found in ANSYS FLUENT 2020 R1.

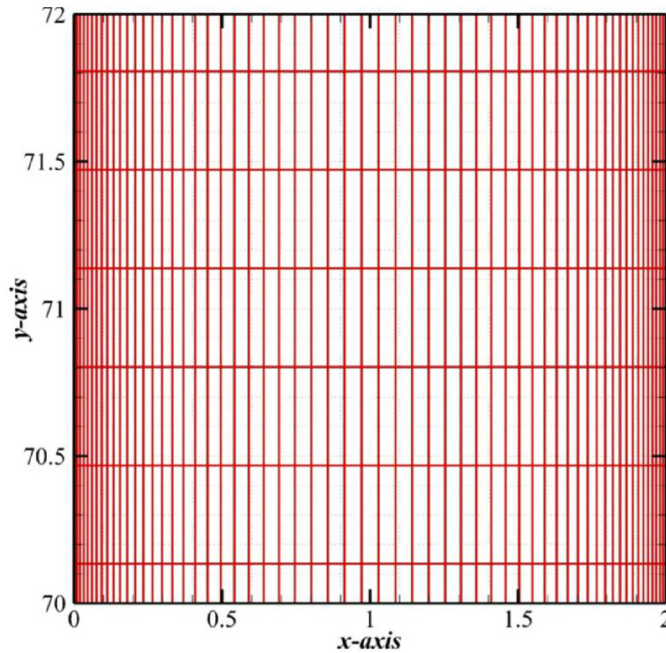
### 3.5 Numerical methods

Figure 10 shows the computational domain and a structured grid system. It should be noted that only the  $y$ -axis region from 70 to 72 mm and the  $x$ -axis region from 0 to 2 mm are plotted. To guarantee the accuracy of the simulation, enhanced wall treatment is employed in the region near the wall, and  $y^+$  is less than unity. The governing equations are discretized and iteratively solved by the finite volume method. The second-order upwind difference scheme is used to spatially discretize the relevant variations. The pressure-velocity coupling is realized by the function of coupled. The stiff chemistry solver was used for the chemistry solver. The turbulence-chemistry interaction is solved by the eddy-dissipation concept. The spatial discretization of reactants and products was conducted by the first-order upwind scheme. The FLUENT 2020 R1 is used, and the simulation is considered to be converged when the residuals reach  $10^{-5}$ .

## 4. Numerical assessment

### 4.1 Study of the turbulence models

The RANS model is used to analyze the thermo-hydrodynamic characteristics. Based on the open published literature (Zhao *et al.*, 2017; Han *et al.*, 2018), the low Reynolds number SST  $k-\omega$  is suitable to simulate the supercritical thermal transport. To further validate the rationality and reliability of numerical simulations, the numerical results are compared with tested measurements (Liu *et al.*, 2015) in which the n-decane flowing upward in a round tube was investigated. Figure 11 depicts the numerical results with SST  $k-\omega$ . Thermal pyrolysis was considered in one case while it was not considered in another case. Also, the inner wall temperature from the experiment was shown in Figure 11. As was expected, the numerical results with thermal pyrolysis are better than those without thermal pyrolysis. However, the HTD phenomenon was brought forward. From the



**Figure 10.** Discretization of the computational domain and the initial mesh height and growth rate are 0.01 mm and 1.05, respectively

location of  $x/d_{in} = 93.5$  to the  $x/d_{in} = 366.3$  (the last measurement point along the tube), the maximum deviation between the experimental data and numerical data is 7.0%, and this indicates that the SST  $k-\omega$  is appropriate for the study of the supercritical thermal transport coupling with thermal cracking. Nevertheless, it needs to be declared that the cause of the deviation is closely relevant to the precision of thermo-physical properties and chemical cracking reactions.

#### 4.2 Study of the mesh sensitivity

It was illustrated in Section 3.5 that the computational domain should be discretized by a structured mesh before the numerical simulation. Four sets of grids were drawn, and the outlet average temperature and velocity [these expressions are shown in equations (11) and (12)] were used to confirm the finest grid settings. As shown in Table 3, the mesh numbers of 15,900, 25,000, 39,000, 51,000 were detected, and it is reported that the mesh number of 39,000 was suitable to study the conjugation between thermal transport and cracking, and the deviations of the outlet average temperature and velocity are  $-0.17$  and  $0.32\%$ , respectively, by comparing with the results in the case with a mesh number of 51,000.

$$T_b = \frac{\int_A \rho u c_p T dA}{\int_A \rho u c_p dA} \quad (11)$$

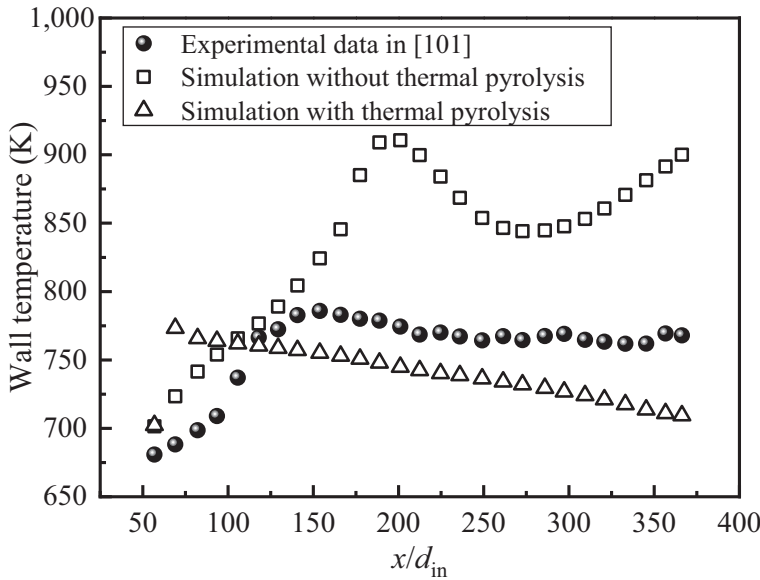


**Figure 11.**  
Validation of  
turbulence models to  
the supercritical  
hydrocarbon fuel  
n-decane flowing  
upward in a vertically  
placed circular pipe

Cases	Mesh no.	Outlet average temperature (K)	Outlet average velocity (m/s)	Temperature/velocity deviation
Case 1	15,900	522.8	1.57	-0.15%/0
Case 2	25,000	523.2	1.56	-0.08%/-0.6%
Case 3	39,000	522.7	1.575	-0.17%/0.32%
Case 4	51,000	523.6	1.57	Criterion

**Table 3.**  
Validation of the  
mesh sensitivity  
based on four sets of  
meshes

$$v_{ave} = \frac{1}{A} \int_A u dA \quad (12)$$

## 5. Results and discussion

### 5.1 The heated wall temperature

In the supercritical heat transfer, the wall temperature distribution is commonly used to determine if the HTD and HTE phenomena will happen (Edwards, 2003; Hobold and Silva, 2016). In this study, the wall temperature distributions of the case without thermal pyrolysis and the case with thermal pyrolysis are demonstrated in Figure 12. It is found that the wall temperature with thermal cracking is lower than that without thermal cracking. Furthermore, near the region of  $y = 100$  mm, an HTD phenomenon appears when the thermal pyrolysis is not considered, while an HTE phenomenon occurs when the thermal cracking is involved. This implies that the cracking can effectively decrease the wall temperature of the combustor. In the initial stages of heat transfer, i.e. before the position of  $y = 32$  mm, the wall temperatures of the two cases are the same because the thermal pyrolysis occurs when the temperature is larger than 770 K (Jia et al., 2014). It is clearly

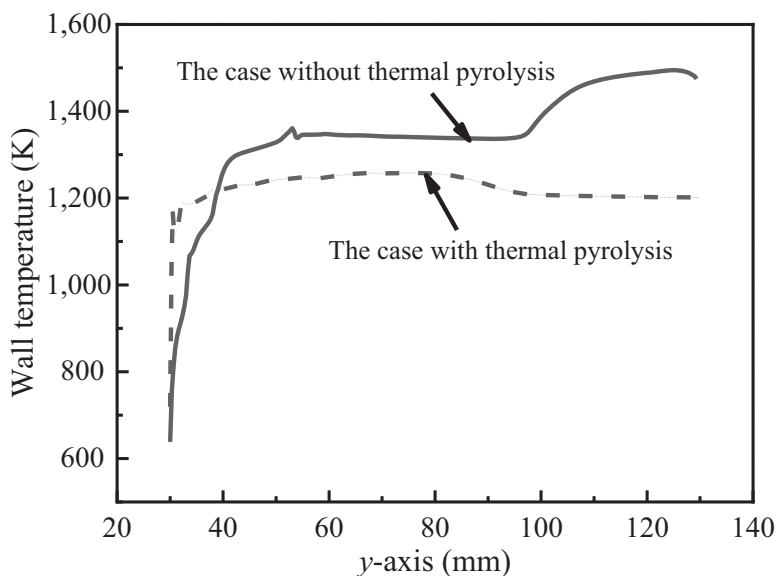
found that the wall temperature is smaller than 770 K before the position of  $y = 32$  mm. Also, this phenomenon indirectly proves the accuracy of the numerical simulation.

### 5.2 Distribution of $y$ -axis velocity

It is common sense that the thermal transport is relevant to the flow characteristics. Figure 13 compared the  $y$ -axis velocity distributions between the case with thermal pyrolysis and the case without thermal pyrolysis. It is found that the average  $y$ -axis velocity of the fluid is increased by the thermal pyrolysis particularly in the vicinity of the outlet region. This is an important reason corresponding to the reduced temperature under the participation of thermal pyrolysis as shown in Figure 12. Also, the thermal pyrolysis increases the gradient of the  $y$ -axis velocity along with the mainstream, implying that the acceleration is generated by the large gradient of the density, which enhances heat transfer, i.e. decreasing the wall temperature. There are two reasons for the change in density. The first one is the dramatic variation of supercritical hydrocarbon fuel and the second one is the generation of the new product due to the thermal pyrolysis. The dramatic variation of supercritical hydrocarbon fuel has been widely introduced and only the effects of reactant and product distribution on the density of the hydrocarbon fuel were studied in this work.

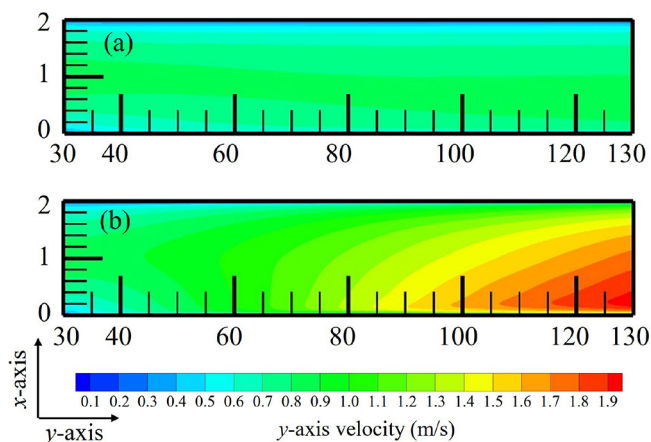
### 5.3 The effects of reactant and product distribution

Figure 14 gives the cracking rate of  $n$ -decane at the exit section along the  $x$ -axis. It can be seen that the average cracking rate is 13%, and it is less than 20% (PPD model proposed is valid within 20% as shown in Table 2). However, the maximum cracking rate at the exit section is 26% (the position near the heated wall) and it is slightly larger than 20%. In Zhang (2016), it is reported that the PPD model proposed by Ward *et al.* can be extended with cracking rate of 76%, thus it is still used in this work. Figure 15 plots the mass fractions of  $C_{10}H_{22}$  (reactant) and  $C_6H_{12}$  (product) for the case with thermal pyrolysis, respectively. It is found that the mass fraction of  $C_{10}H_{22}$  decreases with the flow direction due to the thermal



**Figure 12.**  
Comparison of the wall temperature for the case without thermal pyrolysis and the case with thermal pyrolysis

pyrolysis, especially, in the zone near the heated plane. Accordingly, the mass fraction of products such as  $C_6H_{12}$  increases along the mainstream in the vicinity of the heated plane. This means that more small molecules are produced and the small density of the mixture (reactant and products) is caused as shown in Figure 16. In comparison to the case without thermal pyrolysis, a larger variation of density can be found in the case with thermal pyrolysis. This implies that the dramatic variation of density caused by thermal pyrolysis is dominant in the thermal-induced acceleration. By comparing Figures 15 and 16, it is found that the change of the density coincides with the production of small molecules. This further confirms that the generation of acceleration is driven by the drastic density change because of the thermal pyrolysis.



**Figure 13.**  
The y-axis velocity  
distributions for  
(a) the case without  
thermal pyrolysis and  
(b) the case with  
thermal pyrolysis,  
respectively

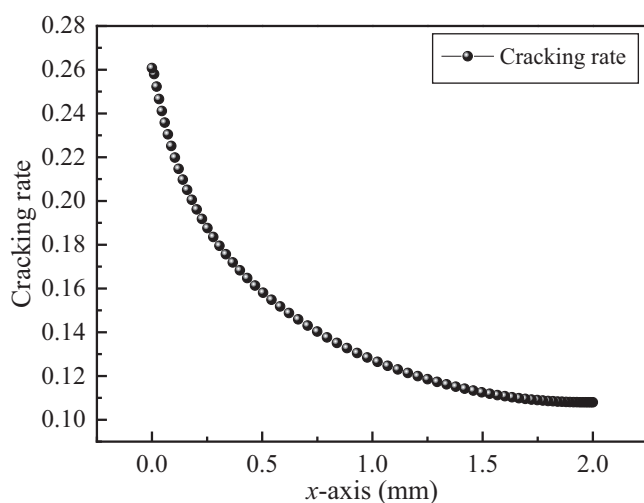


**Figure 14.**  
The cracking rate of  
n-decane at the exit  
section along the  
x-axis

### 6. Conclusions

Supercritical fuel cooling is an excellent way to decrease the wall temperature of the combustor in a scramjet engine. In the cooling process, HTD and HTE can be observed. Furthermore, the thermal pyrolysis phenomenon can also be found with an increase of fluid temperature. Regarding these issues, a brief review of current research on supercritical aviation kerosene phenomena was organized first in views of the surrogate model of hydrocarbon fuels, chemical cracking mechanism of hydrocarbon fuels, thermo-physical properties of hydrocarbon fuels, turbulence model, flow characteristics and thermal performances. Then, numerical simulations were implemented to study the supercritical thermal transport of n-decane with thermal pyrolysis. The properties of the reactant and the pyrolysis products were calculated by the ASPEN HYSYS. The PPD chemical

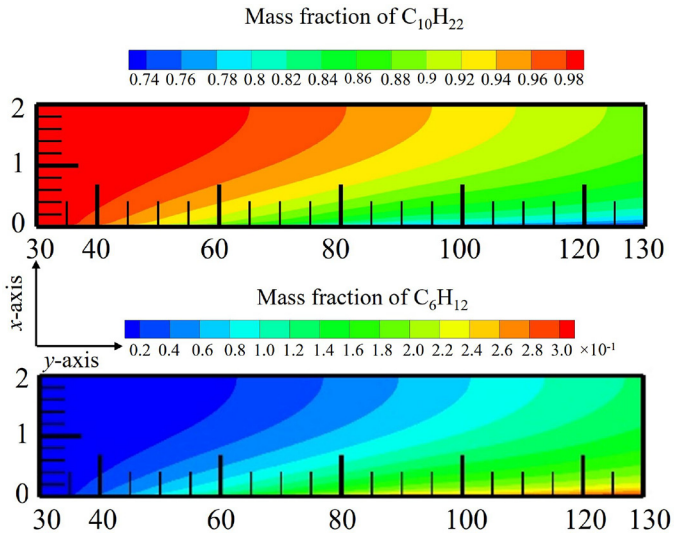


**Figure 15.** The mass fractions of  $C_{10}H_{22}$  (reactant) and  $C_6H_{12}$  (product) for the case with thermal pyrolysis

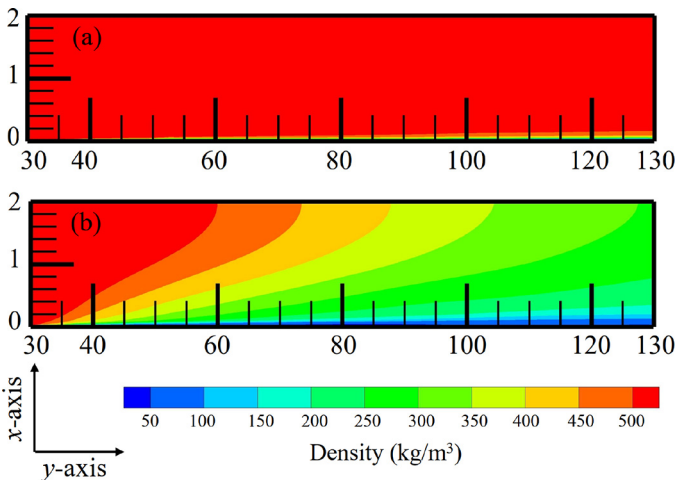


**Figure 16.** The density distributions for (a) the case without thermal pyrolysis and (b) the case with thermal pyrolysis, respectively

cracking mechanism was applied. The SST  $k-\omega$  was used because it has relatively high precisions. Based on the above contents, some findings are summarized as follows:

- The surrogate model and chemical cracking mechanism of hydrocarbon fuels are the key steps to explore the thermo-hydrodynamic characteristics of supercritical aviation kerosene. The existing models have corresponding application scope, which should be paid more attention to.
- The thermo-physical properties of existing surrogate models of aviation kerosene cannot match well with the experimental data. Also, quite different thermo-physical properties are obtained from SUPERTRAPP, Aspen HYSYS, Aspen Plus and REFPROP, and in-house code based on the extended corresponding state principle. This issue should be noticed.
- The modification of turbulence models is only based on the existing turbulence models and more work should be implemented to enhance the prediction accuracy of thermo-hydrodynamic characteristics of supercritical fluids.
- Numerous experimental studies were dedicated to studying the thermo-hydrodynamic characteristics of supercritical aviation kerosene and thermal pyrolysis. However, the coupling influence mechanism between the convective heat transfer and thermal pyrolysis is difficult to explain by the experimental data. Thus, it is necessary to numerically investigate the impact of thermal pyrolysis on thermal transport. Based on this study, the wall temperature of the combustion chamber can be effectively reduced by thermal pyrolysis, i.e. the HTD phenomenon can be attenuated or suppressed by thermal pyrolysis. This is because the thermal-induced acceleration is driven by the drastic density change, which is caused by the production of small molecules. This reason is more important than the properties of the reactant and products.

## References

- Abe, K., Kondoh, T. and Nagano, Y. (1994), "A new turbulence model for predicting fluid flow and heat transfer in separating and reattaching flows-I. Flow field calculations", *International Journal of Heat and Mass Transfer*, Vol. 37 No. 1, pp. 139-151.
- Bae, J.H. and Yoo, J.Y. (2005), "Direct numerical simulation of turbulent supercritical flows with heat transfer", *Physics of Fluids*, Vol. 17 No. 10, pp. 465-488.
- Bao, W., Li, X.L., Qin, J., Zhou, W.X. and Yu, D.R. (2012), "Efficient utilization of heat sink of hydrocarbon fuel for regeneratively cooled scramjet", *Applied Thermal Engineering*, Vols 33/34, pp. 208-218.
- Bao, W., Zhang, S.L., Qin, J., Zhou, W.X. and Xie, K.L. (2014), "Numerical analysis of flowing cracked hydrocarbon fuel inside cooling channels in view of thermal management", *Energy*, Vol. 67, pp. 149-161.
- CHEMKIN-PRO 15092 (2009), Reaction Design, CHEMKIN-PRO 15092, San Diego, CA.
- Chen, Y.Q., Li, Y., Sundén, B. and Xie, G.N. (2020), "The abnormal heat transfer behavior of supercritical n-decane flowing in a horizontal tube under regenerative cooling for scramjet engines", *Applied Thermal Engineering*, Vol. 167, paper no: 114637.
- Cheng, D., Wang, X.Z. and Fan, X.J. (2012), "Study on thermal physical surrogate model of kerosene RP-3", *Hypersonic Symposium and the 5th National Conference on Hypersonic Science and Technology*, Paper No. CSTAM2012-B03-0280.
- Cheng, Z.Y., Tao, Z., Zhu, J.Q. and Wu, H.W. (2018), "Diameter effect on the heat transfer of supercritical hydrocarbon fuel in horizontal tubes under turbulent conditions", *Applied Thermal Engineering*, Vol. 134, pp. 39-53.

- Cheng, Z.Y., Zhu, J.Q. and Jin, Z. (2016), "Study on surrogate model of endothermic hydrocarbon fuel RP-3", *Chinese Journal of Aerospace Power*, Vol. 31, pp. 391-398.
- Dagaut, P. and Cathonnet, M. (2006), "The ignition, oxidation, and combustion of kerosene: a review of experimental and kinetic modeling", *Progress in Energy and Combustion Science*, Vol. 32 No. 1, pp. 48-92.
- Dahm, K.D., Virk, P.S., Bounaceur, R., Battin-Leclerc, F., Marquaire, P.M., Fournet, R., Daniau, E. and Bouchez, M. (2004), "Experimental and modelling investigation of the thermal decomposition of n-dodecane", *Journal of Analytical and Applied Pyrolysis*, Vol. 71 No. 2, pp. 865-881.
- Daniau, E., Bouchez, M., Herbinet, O., Marquaire, P.M., Gascoin, N. and Gillard, P. (2005), "Fuel reforming for scramjet thermal management and combustion optimization", *AIAA/CIRA 13th International Space Planes and Hypersonics Systems and Technologies*, paper no. AIAA 2005-3403.
- Deng, H.W., Zhang, C.B., Xu, G.Q., Tao, Z., Zhang, B. and Liu, G.Z. (2011), "Density measurements of endothermic hydrocarbon fuel at sub- and supercritical conditions", *Journal of Chemical and Engineering Data*, Vol. 56 No. 6, pp. 2980-2986.
- Deng, H.W., Zhu, K., Xu, G.Q., Tao, Z., Zhang, C.B. and Liu, G.Z. (2012a), "Isobaric heat capacity measurement for kerosene RP-3 in the near-critical and supercritical regions", *Journal of Chemical and Engineering Data*, Vol. 57 No. 2, pp. 263-268.
- Deng, H.W., Zhang, C.B., Xu, G.Q., Zhang, B., Tao, Z. and Zhu, K. (2012b), "Viscosity measurements of endothermic hydrocarbon fuel from (298 to 788) K under supercritical pressure conditions", *Journal of Chemical and Engineering Data*, Vol. 57 No. 2, pp. 358-365.
- Edwards, T. (2006), "Cracking and deposition behavior of supercritical hydrocarbon aviation fuels", *Combustion Science and Technology*, Vol. 178, pp. 307-334.
- Edwards, T. (2003), "Liquid fuels and propellants for aerospace propulsion: 1993-2003", *Journal of Propulsion and Power*, Vol. 19 No. 6, pp. 1089-1107.
- Fan, X.J. and Yu, G. (2006), "Analysis of thermophysical properties of daqing RP-3 aviation kerosene", *Chinese Journal of Propulsion Technology*, Vol. 27, pp. 187-192.
- Fan, X.J., Yu, G., Li, J.G., Zhang, X.Y. and Sung, C.J. (2006), "Investigation of vaporized kerosene injection and combustion in a supersonic model combustor", *Journal of Propulsion and Power*, Vol. 22 No. 1, pp. 103-110.
- Fu, Y.C., Huang, H.R., Wen, J., Xu, G.Q. and Zhao, W. (2017a), "Experimental investigation on convective heat transfer of supercritical RP-3 in vertical miniature tubes with various diameters", *International Journal of Heat and Mass Transfer*, Vol. 112, pp. 814-824.
- Fu, Y.C., Wen, J., Tao, Z., Xu, G.Q. and Huang, H.R. (2017b), "Experimental research on convective heat transfer of supercritical hydrocarbon fuel flowing through U-turn tubes", *Applied Thermal Engineering*, Vol. 116, pp. 43-55.
- Gascoin, N., Gillard, P., Bernard, S., Daniau, E. and Bouchez, M. (2008), "Pyrolysis of supercritical endothermic fuel: evaluation for active cooling instrumentation", *International Journal of Chemical Reactor Engineering*, Vol. 6 No. 1, paper no: Article A7.
- Gong, K.Y., Cao, Y., Feng, Y., Liu, S.Y. and Qin, J. (2019), "Influence of secondary reactions on heat transfer process during pyrolysis of hydrocarbon fuel under supercritical conditions", *Applied Thermal Engineering*, Vol. 159, paper no. 113912.
- Han, C.L., Zhang, Y.N., Yu, H., Lu, Y.P. and Jiao, B. (2018), "Numerical analysis on non-uniform flow and heat transfer of supercritical cryogenic methane in a heated horizontal circular tube", *The Journal of Supercritical Fluids*, Vol. 138, pp. 82-91.
- Herbinet, O., Marquaire, P.M., Battin-Leclerc, F. and Fournet, R. (2007), "Thermal decomposition of n-dodecane: experiments and kinetic modeling", *Journal of Analytical and Applied Pyrolysis*, Vol. 78 No. 2, pp. 419-429.
- Hobold, G.M. and Silva, A.K.D. (2016), "Thermal behavior of supercritical fluids near the critical point", *Numerical Heat Transfer, Part A: Applications*, Vol. 69 No. 6, pp. 545-557.

- Hou, L.Y., Dong, N. and Sun, D.P. (2013), "Heat transfer and thermal cracking behavior of hydrocarbon fuel", *Fuel*, Vol. 103, pp. 1132-1137.
- Hu, X.Z., Tao, Z., Zhu, J.Q. and Li, H.W. (2017), "Numerical study of pyrolysis effects on supercritical-pressure flow and conjugate heat transfer of n-decane in the square channel", *Proceedings of ASME Turbo Expo 2017: Turbomachinery Technical Conference and Exposition GT2017*, June 26-30, 2017, Charlotte, NC, USA.
- Huang, D., Ruan, B., Wu, X.Y., Zhang, W., Xu, G.Q., Tao, Z., Jiang, P.X., Ma, L.X. and Li, W. (2015), "Experimental study on heat transfer of aviation kerosene in a vertical upward tube at supercritical pressures", *Chinese Journal of Chemical Engineering*, Vol. 23 No. 2, pp. 425-434.
- Huang, H., Sobel, D.R. and Spadaccini, L.J. (2002), "Endothermic heat-sink hydrocarbon fuels for scramjet cooling", *38th AIAA/ASME/SAE/ASEE Joint Propulsion Conference and Exhibit*, paper no. AIAA 2002-3871.
- Jia, Z.J., Huang, H.Y., Zhou, W.X., Qi, F. and Zeng, M.R. (2014), "Experimental and modeling investigation of n-decane pyrolysis at supercritical pressures", *Energy and Fuels*, Vol. 28 No. 9, pp. 6019-6028.
- Jia, Z.J., Zhou, W.X., Yu, W.L. and Han, Z.X. (2019), "Experimental investigation on pyrolysis of n-decane initiated by nitropropane under supercritical pressure in a miniature tube", *Energy and Fuels*, Vol. 33 No. 6, pp. 5529-5537.
- Jiang, P.X., Wang, Z.C. and Xu, R.N. (2018), "A modified buoyancy effect correction method on turbulent convection heat transfer of supercritical pressure fluid based on RANS model", *International Journal of Heat and Mass Transfer*, Vol. 127, pp. 257-267.
- Jiang, P.X., Yan, J.J., Yan, S., Lu, Z.L. and Zhu, Y.H. (2019), "Thermal cracking and heat transfer of hydrocarbon fuels at supercritical pressures in vertical tubes", *Heat Transfer Engineering*, Vol. 40 Nos 5/6, pp. 437-449.
- Jiang, R.P., Liu, G.Z. and Zhang, X.W. (2013), "Thermal cracking of hydrocarbon aviation fuels in regenerative cooling microchannels", *Energy and Fuels*, Vol. 27 No. 5, pp. 2563-2577.
- Jiao, S., Li, S.F., Pu, H., Dong, M. and Shang, Y. (2018), "Investigation of pressure effect on thermal cracking of n-decane at supercritical pressures", *Energy and Fuels*, Vol. 32 No. 3, pp. 4040-4048.
- Jiao, S., Li, S.F., Pu, H., Dong, M. and Shang, Y. (2020), "Investigation of pyrolysis effect on convective heat transfer characteristics of supercritical aviation kerosene", *Acta Astronautica*, Vol. 171, pp. 55-68.
- Jing, T.T., He, G.Q., Li, W.Q., Zhang, D., Qin, F. and Li, R. (2018), "Flow and thermal analyses of supercritical hydrocarbon fuel in curved regenerative cooling channel around cavity in rocket based combined cycle engine", *Applied Thermal Engineering*, Vol. 145, pp. 423-434.
- Kim, D.E. and Kim, M.H. (2010), "Experimental study of flow acceleration and buoyancy on heat transfer in a supercritical fluid flow in a circular tube", *Nuclear Engineering and Design*, Vol. 240 No. 10, pp. 3336-3349.
- Lei, Z.L., He, K., Huang, Q., Bao, Z.W. and Li, X.Y. (2020), "Numerical study on supercritical heat transfer of n-decane during pyrolysis in rectangular tubes", *Applied Thermal Engineering*, Vol. 170, paper no. 115002.
- Lenhart, D.B., Miller, D.L. and Cernansky, N.P. (2007), "The oxidation of JP-8, Jet-A, and their surrogates in the low and intermediate temperature regime at elevated pressures", *Combustion Science and Technology*, Vol. 179 No. 5, pp. 845-861.
- Li, J., Jiang, G.M., Yu, H.X. and Yu, J.C. (2016), "Development of turbulence model with density fluctuation for supercritical pressure", *Chinese Atomic Energy Science and Technology*, Vol. 50, pp. 640-644.
- Li, J., Jiang, G.M., Yu, J.Y. and Yu, J.C. (2014), "Performance assessment of turbulence models in CFX for predicting heat transfer of supercritical water", *Chinese Atomic Energy Science and Technology*, Vol. 48, pp. 67-73.
- Li, S.F., Wang, Y.N., Dong, M., Pu, H., Jiao, S. and Shang, Y. (2019a), "Experimental investigation on flow and heat transfer instabilities of RP-3 aviation kerosene in a vertical miniature tube under supercritical pressures", *Applied Thermal Engineering*, Vol. 149, pp. 73-84.

- Li, Z.Z., Wang, H.Y., Jing, K., Wang, L.M., Li, Y., Zhang, X.W. and Liu, G.Z. (2019b), "Kinetics and modeling of supercritical pyrolysis of endothermic hydrocarbon fuels in regenerative cooling channels", *Chemical Engineering Science*, Vol. 207, pp. 202-214.
- Li, Y., Sun, F., Sunden, B. and Xie, G.N. (2019c), "Turbulent heat transfer characteristics of supercritical n-decane in a vertical tube under various operating pressures", *International Journal of Energy Research*, Vol. 43 No. 9, pp. 4652-4669.
- Li, Y., Sun, F., Xie, G.N. and Qin, J. (2018), "Improved thermal performance of cooling channels with truncated ribs for a scramjet combustor fueled by endothermic hydrocarbon", *Applied Thermal Engineering*, Vol. 142, pp. 695-708.
- Li, Y., Sun, F., Xie, G.N. and Sunden, B. (2020), "Numerical analysis of supercritical n-decane upward flow and heat transfer characteristics in the buffer layer of a vertical tube", *Numerical Heat Transfer, Part A: Applications*, Vol. 77 No. 3, pp. 247-265.
- Li, Y., Xie, G.N. and Sunden, B.A. (2021a), "Effect of wall conduction on the heat transfer characteristics of supercritical n-decane in a horizontal rectangular pipe for cooling of a scramjet combustor", *International Journal of Numerical Methods for Heat and Fluid Flow*, Vol. 31 No. 3, pp. 880-896.
- Li, Y., Wang, J.B., Xie, G.N. and Bengt, S. (2021b), "Effect of thermal pyrolysis on heat transfer and upward flow characteristics in a rectangular channel using endothermic hydrocarbon fuel", *Chemical Engineering Science*, Vol. 244, paper no. 116806.
- Liang, C., Wang, Y., Jiang, S.C., Zhang, Q.Y. and Li, X.Y. (2017), "The comprehensive study on hydrocarbon fuel pyrolysis and heat transfer characteristics", *Applied Thermal Engineering*, Vol. 117, pp. 652-658.
- Liu, B., Zhu, Y.H., Yun, J.J., Lei, Y.T., Zhang, B. and Jiang, P.X. (2015), "Experimental investigation of convection heat transfer of n-decane at supercritical pressures in small vertical tubes", *International Journal of Heat and Mass Transfer*, Vol. 91, pp. 734-746.
- Liu, P.H., Zhang, T.H., Zhou, L.X., Chen, Z.C., Zhu, Q., Wang, J.L. and Li, X.Y. (2019a), "Experimental and numerical analysis on flow characteristics and pyrolysis mechanism of hydrocarbon fuel with a novel online hybrid method", *Energy Conversion and Management*, Vol. 198, paper no. 111817.
- Liu, Z.G., Zhang, Z.J., Zhao, S.J., Pan, H. and Bi, Q.C. (2019b), "Heat transfer of supercritical endothermic fuel in 3-mm diameter channels: comparison between asymmetric and uniform heating", *International Journal of Heat and Mass Transfer*, Vol. 140, pp. 371-378.
- Mawid, M.A., Park, T.W., Sekar, B. and Arana, C.A. (2003), "Development of detailed chemical kinetic mechanisms for ignition/oxidation of JP-8/Jet-A/JP-7 fuels", *Proceedings of ASME Turbo Expo*, Atlanta, GA, paper no. GT2003-38932.
- Negoescu, C.C., Li, Y.L., Duri, B.A. and Ding, Y.L. (2017), "Heat transfer behaviour of supercritical nitrogen in the large specific heat region flowing in a vertical tube", *Energy*, Vol. 134, pp. 1096-1106.
- Niceno, B. and Sharabi, M. (2013), "Large eddy simulation of turbulent heat transfer at supercritical pressures", *Nuclear Engineering and Design*, Vol. 261, pp. 44-55.
- NIST (1999), NIST thermophysical properties of hydrocarbon mixtures database: version 3.0, NIST Standard Reference Database 4, Gaithersburg, MD, National Institute of Standards and Technology.
- Pei, X.Y. and Hou, L.Y. (2017), "Effect of different species on physical properties for the surrogate fuel", *Chinese Journal of Tsinghua University*, Vol. 57, pp. 774-779.
- Petukhov, B.S., Polyakof, A.F., Kuleshov, V.A. and Shekter, Y.L. (1974), "Turbulent flow and heat transfer in horizontal tubes with substantial influence of thermo-gravitational forces", *Proceedings of Fifth International Heat Transfer Conference*, pp. 3-7.
- Pizzarelli, M., Nasuti, F. and Onofri, M. (2016), "Evolution of cooling-channel properties for varying aspect ratio", *Progress in Propulsion Physics*, Vol. 8, pp. 117-128.

- Pu, H., Dong, M., Li, S.F., Jiao, S. and Shang, Y. (2019), "Application of four-equation closure for turbulent heat flux in prediction of convective heat transfer to hydrocarbon fuels at supercritical pressures", *International Journal of Thermal Sciences*, Vol. 143, pp. 37-51.
- Qin, J., Zhang, S.L., Bao, W., Yu, W.L., Yu, B., Zhou, W.X. and Yu, D.R. (2013), "Experimental study on chemical recuperation process of endothermic hydrocarbon fuel", *Fuel*, Vol. 108, pp. 445-450.
- Rao, P.N. and Kunzru, D. (2006), "Thermal cracking of JP-10: kinetics and product distribution", *Journal of Analytical and Applied Pyrolysis*, Vol. 76 Nos 1/2, pp. 154-160.
- Ren, Y.Z., Zhu, J.Q. and Deng, H.W. (2013), "Numerical study of heat transfer of RP-3 at supercritical pressure", *Advanced Materials Research*, Vol. 663, pp. 470-476.
- Ruan, B., Meng, H. and Yang, V. (2014), "Simplification of pyrolytic reaction mechanism and turbulent heat transfer of n-decane at supercritical pressures", *International Journal of Heat and Mass Transfer*, Vol. 69, pp. 455-463.
- Sun, X., Xu, K.K. and Meng, H. (2018a), "Supercritical-pressure heat transfer, pyrolytic reactions, and surface coking of n-decane in helical tubes", *Energy and Fuels*, Vol. 32 No. 12, pp. 12298-12307.
- Sun, X., Xu, K.K. and Meng, H. (2018b), "Supercritical-pressure heat transfer of n-decane with fuel pyrolysis in helical tube", *CIESC Journal*, Vol. 69, pp. 20-25.
- Sunden, B.A., Wu, Z. and Huang, D. (2016), "Comparison of heat transfer characteristics of aviation kerosene flowing in smooth and enhanced mini tubes at supercritical pressures", *International Journal of Numerical Methods for Heat and Fluid Flow*, Vol. 26 Nos 3/4, pp. 1289-1308.
- Tao, Z., Hu, X.Z., Zhu, J.Q. and Wu, H.W. (2018a), "Numerical investigation of pyrolysis effects on heat transfer characteristics and flow resistance of n-decane under supercritical pressure", *Chinese Journal of Aeronautics*, Vol. 31 No. 6, pp. 1249-1257.
- Tao, Z., Cheng, Z.Y., Zhu, J.Q., Hu, X.Z. and Wang, L.Y. (2018b), "Correction of low-Reynolds number turbulence model to hydrocarbon fuel at supercritical pressure", *Aerospace Science and Technology*, Vol. 77, pp. 156-167.
- Tao, Z., Li, L.W., Zhu, J.Q., Hu, X.Z., Wang, L.Y. and Qiu, L. (2019), "Numerical investigation on flow and heat transfer characteristics of supercritical RP-3 in inclined pipe", *Chinese Journal of Aeronautics*, Vol. 32 No. 8, pp. 1885-1894.
- TsujiKawa, Y. and Northam, G.B. (1996), "Effects of hydrogen active cooling on scramjet engine performance", *International Journal of Hydrogen Energy*, Vol. 21 No. 4, pp. 299-304.
- Violi, A., Yan, S., Eddings, E.G., Sarofim, A.F., Granata, S., Faravelli, T. and Ranzi, E. (2002), "Experimental formulation and kinetic model for JP-8 surrogate mixtures", *Combustion Science and Technology*, Vol. 174 Nos 11/12, pp. 399-417.
- Wang, Y.H., Li, S.F. and Dong, M. (2019), "Experimental investigation on heat transfer deterioration and thermo-acoustic instability of supercritical-pressure aviation kerosene within a vertical upward circular tube", *Applied Thermal Engineering*, Vol. 157, paper no. 113707.
- Wang, Y.Z., Hua, Y.X. and Meng, H. (2010), "Numerical studies of supercritical turbulent convective heat transfer of cryogenic-propellant methane", *Journal of Thermophysics and Heat Transfer*, Vol. 24 No. 3, pp. 490-500.
- Wang, Y., Zhao, Y., Liang, C., Chen, Y., Zhang, Q.Y. and Li, X.Y. (2017), "Molecular-level modeling investigation of n-decane pyrolysis at high temperature", *Journal of Analytical and Applied Pyrolysis*, Vol. 128, pp. 412-422.
- Ward, T.A., Ervin, J.S., Striebich, R.C. and Zabarnick, S. (2004), "Simulations of flowing mildly cracked normal alkanes incorporating proportional product distributions", *Journal of Propulsion and Power*, Vol. 20 No. 3, pp. 394-402.
- Ward, T.A., Ervin, J.S., Zabarnick, S. and Shafer, L. (2005), "Pressure effects on flowing mildly cracked n-decane", *Journal of Propulsion and Power*, Vol. 21 No. 2, pp. 344-355.

- Wen, J., Huang, H.R., Jia, Z.X., Fu, Y.C. and Xu, G.Q. (2017a), "Buoyancy effects on heat transfer to supercritical pressure hydrocarbon fuel in a horizontal miniature tube", *International Journal of Heat and Mass Transfer*, Vol. 115, pp. 1173-1181.
- Wen, J., Huang, H.R., Fu, Y.C., Xu, G.Q. and Zhu, K. (2017b), "Heat transfer performance of aviation kerosene RP-3 flowing in a vertical helical tube at supercritical pressure", *Applied Thermal Engineering*, Vol. 121, pp. 853-862.
- Wen, Q.L. and Gu, H.Y. (2010), "Numerical simulation of heat transfer deterioration phenomenon in supercritical water through vertical tube", *Annals of Nuclear Energy*, Vol. 37 No. 10, pp. 1272-1280.
- Xiao, B.G., Yang, S.H., Zhao, H.Y., Qian, W.Q. and Le, J.L. (2010), "Detailed and reduced chemical kinetic mechanisms for RP-3 aviation kerosene combustion", *Chinese Journal of Aerospace Power*, Vol. 25, pp. 1948-1955.
- Xie, G.N., Xu, X.X., Lei, X.L., Li, Z.H., Li, Y. and Sunden, B. (2021), "Heat transfer behaviors of some supercritical fluids: a review", *Chinese Journal of Aeronautics*.
- Xing, Y., Xie, W.J., Fang, W.J., Guo, Y.S. and Lin, R.S. (2009), "Kinetics and product distributions for thermal cracking of kerosene-based aviation fuel", *Energy and Fuels*, Vol. 23 No. 8, pp. 4021-4024.
- Xu, K.K. and Meng, H. (2015a), "Modeling and simulation of supercritical-pressure turbulent heat transfer of aviation kerosene with detailed pyrolytic chemical reactions", *Energy and Fuels*, Vol. 29 No. 7, pp. 4137-4149.
- Xu, K.K. and Meng, H. (2015b), "Analyses of surrogate models for calculating thermophysical properties of aviation kerosene RP-3 at supercritical pressures", *Science China Technological Sciences*, Vol. 58 No. 3, pp. 510-518.
- Xu, K.K. and Meng, H. (2016), "Numerical study of fluid flows and heat transfer of aviation kerosene with consideration of fuel pyrolysis and surface coking at supercritical pressures", *International Journal of Heat and Mass Transfer*, Vol. 95, pp. 806-814.
- Xu, K.K., Ruan, B. and Meng, H. (2018a), "Validation and analyses of RANS CFD models for turbulent heat transfer of hydrocarbon fuels at supercritical pressures", *International Journal of Thermal Sciences*, Vol. 124, pp. 212-226.
- Xu, K.K., Sun, X. and Meng, H. (2018b), "Conjugate heat transfer, endothermic fuel pyrolysis and surface coking of aviation kerosene in ribbed tube at supercritical pressure", *International Journal of Thermal Sciences*, Vol. 132, pp. 209-218.
- Yang, C.G., Quan, Z.J., Chen, Y., Zhu, Q., Wang, J.L. and Li, X.Y. (2020), "A comprehensive investigation of the pyrolysis effect on heat transfer characteristics for n-decane in the horizon mini-channel", *Energy and Fuels*, doi: [10.1021/acs.energyfuels.9b03428](https://doi.org/10.1021/acs.energyfuels.9b03428).
- Zeng, W., Li, H.X., Ma, H.A., Liang, S. and Chen, B.D. (2014), "Reduced chemical reaction mechanism of surrogate fuel for RP-3 kerosene", *Chinese Journal of Propulsion Technology*, Vol. 35, pp. 1139-1145.
- Zhang, C.B., Xu, G.Q., Gao, L., Tao, Z., Deng, H.W. and Zhu, K. (2012), "Experimental investigation on heat transfer of a specific fuel (RP-3) flows through downward tubes at supercritical pressure", *The Journal of Supercritical Fluids*, Vol. 72, pp. 90-99.
- Zhang, R.L., Zhao, G.Z., Le, J.L., Huang, W.M., Tong, Z.R. and Xu, X.J. (2015), "Numerical studies for heat transfer of hydrocarbon fuel with thermal cracking", *AIAA International Space Planes and Hypersonic Systems and Technologies Conference*, paper no. AIAA 2015-3621.
- Zhang, S.L. (2016), "Research on the characteristics of regenerative and film cooling for hydrocarbon fueled scramjet engines", Ph.D. Thesis, Harbin Institute of Technology.
- Zhang, S.L., Cui, N.G., Xiong, Y.F., Feng, Y., Qin, J. and Bao, W. (2017), "Effect of channel aspect ratio on chemical recuperation process in advanced aeroengines", *Energy*, Vol. 123, pp. 9-19.
- Zhao, G.Z., Song, W.Y. and Zhang, R.L. (2015), "Effect of pressure on thermal cracking of China RP-3 aviation kerosene under supercritical conditions", *International Journal of Heat and Mass Transfer*, Vol. 84, pp. 625-632.

- 
- Zhao, H.J., Li, X.W. and Wu, X.X. (2017), "Numerical investigation of supercritical water turbulent flow and heat transfer characteristics in vertical helical tubes", *The Journal of Supercritical Fluids*, Vol. 127, pp. 48-61.
- Zhao, Y., Wang, Y., Liang, G., Zhang, Q.Y. and Li, X.Y. (2018), "Heat transfer analysis of n-decane with variable heat flux distributions in a mini-channel", *Applied Thermal Engineering*, Vol. 144, pp. 695-701.
- Zheng, D., Yu, M.W. and Zhong, B.J. (2015), "RP-3 aviation kerosene surrogate fuel and the chemical reaction kinetic model", *Acta Physico-Chimica Sinica*, Vol. 31, pp. 636-642.
- Zhong, F.Q., Fan, X.J., Yu, G. and Li, J.G. (2009b), "Thermal cracking of aviation kerosene for scramjet applications", *Science in China Series E: Technological Sciences*, Vol. 52 No. 9, pp. 2644-2652.
- Zhong, F.Q., Fan, X.J., Yu, G., Li, J.G. and Sung, C.J. (2009a), "Heat transfer of aviation kerosene at supercritical conditions", *Journal of Thermophysics and Heat Transfer*, Vol. 23 No. 3, pp. 543-550.
- Zhou, H., Gao, X.K., Liu, P.H., Zhu, Q., Wang, J.L. and Li, X.Y. (2017), "Energy absorption and reaction mechanism for thermal pyrolysis of n-decane under supercritical pressure", *Applied Thermal Engineering*, Vol. 112, pp. 403-412.
- Zhu, K., Xu, G.Q., Tao, Z., Deng, H.W., Ran, Z.H. and Zhang, C.B. (2013), "Flow frictional resistance characteristics of kerosene RP-3 in horizontal circular tube at supercritical pressure", *Experimental Thermal and Fluid Science*, Vol. 44, pp. 245-252.
- Zhu, Y.H., Liu, B. and Jiang, P.X. (2014), "Experimental and numerical investigations on n-decane thermal cracking at supercritical pressures in a vertical tube", *Energy and Fuels*, Vol. 28 No. 1, pp. 466-474.

**Corresponding author**

Bengt Ake Sundén can be contacted at: [bengt.sunden@energy.lth.se](mailto:bengt.sunden@energy.lth.se)

---

For instructions on how to order reprints of this article, please visit our website:

[www.emeraldgroupublishing.com/licensing/reprints.htm](http://www.emeraldgroupublishing.com/licensing/reprints.htm)

Or contact us for further details: [permissions@emeraldinsight.com](mailto:permissions@emeraldinsight.com)